PalZ
https://doi.org/10.1007/s12542-024-00687-9

RESEARCH PAPER

The Picocoraciades (hoopoes, rollers, woodpeckers, and allies) from the early Eocene London Clay of Walton-on-the-Naze

Gerald Mayr[1] · **Andrew C. Kitchener**[2,3]

Received: 14 December 2023 / Accepted: 4 March 2024

Abstract

We describe upupiform, coraciiform, and possible piciform birds from the early Eocene London Clay of Walton-on-the-Naze (Essex, UK). The material includes partial skeletons of a new species of a small upupiform bird, *Waltonirrisor tendringensis*, gen. et sp. nov., which is the earliest known representative of the Upupiformes. Three very similar species of stem group rollers are assigned to *Laputavis robusta*, *Septencoracias morsensis*, and *S. simillimus*, sp. nov. These species only differ in minor features, which raises the possibility that the taxon *Sepencoracias* Bourdon, 2016 is a junior synonym of *Laputavis* Dyke, 2001. A smaller stem group roller from Walton-on-the-Naze resembles the North American primobucconid species *Primobucco mcgrewi*. We also describe two species of a new genus-level taxon, *Pristineanis*, gen. nov., which shows close affinities to the North American "*Neanis*" *kistneri* and may be a stem group representative of the Piciformes. In many aspects of their postcranial osteology, the stem group Coracii from Walton-on-the-Naze, as well as the new taxon *Pristineanis,* resemble coeval Trogoniformes from this fossil site. Because trogons are the extant sister taxon of the Picocoraciades – the clade including the Upupiformes, Coraciiformes, and Piciformes –, the shared similarities are likely to be plesiomorphic for this latter clade. Early Cenozoic representatives of the Upupiformes and Coraciiformes were much smaller than their extant relatives, which suggests that the Picocoraciades are an avian example of Cope's Rule that postulates a tendency for size increase in evolutionary lineages over time.

Keywords Aves · Evolution · Fossils birds · Systematics · Taxonomy

Introduction

The avian clade Picocoraciades (sensu Sangster et al. 2022; "Picocoraciae" of Mayr 2011) includes three major subclades: Bucerotes (hornbills, hoopoes, and wood hoopoes), Coraciiformes (rollers, bee-eaters, kingfishers and allies), and Piciformes (jacamars, puffbirds, woodpeckers and allies). The former two have a fairly rich Eocene record (Mayr 2022a), but most published fossils stem from only two localities, i.e. the latest early to earliest middle Eocene site Messel in Germany and the early Eocene Green River Formation in Wyoming (USA).

Extant Bucerotes comprise the Bucerotiformes (hornbills) and the Upupiformes, the clade formed by the Upupidae (hoopoes) and Phoeniculidae (wood hoopoes). All early Eocene Bucerotes are currently assigned to the Messelirrisoridae, which are very small stem group representatives of the Upupiformes. Except for a fragmentary humerus of a messelirrisorid from the middle Eocene German locality Geiseltal (Mayr 2002, 2020), all published early/middle Eocene fossils of these birds stem from Messel (Mayr 1998, 2000, 2006).

The Coraciiformes have a more comprehensive record, which comes from Messel, the Green River Formation, and a few other early Cenozoic localities in Europe and North America (Mayr 2022a). The Primobucconidae, which are early diverging stem group representatives of the Coracii (rollers), are represented both in Messel and the Green River

Handling Editor: Ursula Göhlich.

✉ Gerald Mayr
Gerald.Mayr@senckenberg.de

[1] Ornithological Section, Senckenberg Research Institute and Natural History Museum Frankfurt, Senckenberganlage 25, 60325 Frankfurt am Main, Germany

[2] Department of Natural Sciences, National Museums Scotland, Chambers Street, Edinburgh EH1 1JF, UK

[3] School of Geosciences, University of Edinburgh, Drummond Street, Edinburgh EH8 9XP, UK

Published online: 10 April 2024

Formation (Mayr et al. 2004; Ksepka and Clarke 2010). Two more "modern-type" taxa of the Coracii – *Eocoracias brachyptera* and *Paracoracias occidentalis* – likewise occur in Messel and the Green River Formation, respectively (Mayr and Mourer-Chauviré 2000; Clarke et al. 2009). Another early Cenozoic coraciiform bird is *Septencoracias* from the early Eocene Fur Formation in Denmark (Bourdon et al. 2016), which is known from a well-preserved partial skeleton. A tarsometatarsus from the early Eocene of Belgium was tentatively assigned to *Septencoracias morsensis* by Mayr and Smith (2019).

The early Eocene deposits of the British London Clay also yielded a number of fossils that belong to the Picocoraciades, but even though some have been previously figured (Mayr 1998, 2022a), only a few fossils were formally described. Mayr (2022b) reported a record of *Septencoracias* from Walton-on-the-Naze (Essex, UK), and a stem group representative of the Coracii was also found in the London Clay of the Isle of Sheppey (Mayr and Walsh 2018).

Here we describe upupiform and coraciiform birds from Walton-on-the-Naze, which stem from the collection of the late Michael Daniels and represent the richest assemblage of the Picocoraciades from the London Clay known to date. The material consists of multiple well-preserved partial skeletons and informs the osteology of early Eocene Upupiformes and Coracii. The roller fossils also

◂**Fig. 1** Specimens of the upupiform bird *Waltonirrisor tendringensis*, gen. et sp. nov. from the early Eocene London Clay of Walton-on-the-Naze (Essex, UK) in comparison to crown group Upupiformes. **a–g** overview of the fossils (**a** NMS.Z.2021.40.134, **b** NMS.Z.2021.40.136, **c** NMS.Z.2021.40.137, **d** NMS.Z.2021.40.138, **e** NMS.Z.2021.40.140, **f** NMS.Z.2021.40.135, **g** NMS.Z.2021.40.139). **h**, **i** *W. tendringensis*, gen. et sp. nov. (NMS.Z.2021.40.137), rostral portion of mandible in ventral (**h**) and dorsal (**i**) view. **j–l** *W. tendringensis*, gen. et sp. nov. (NMS.Z.2021.40.137), caudal portion of right mandibular ramus in lateral (**j**), medial (**k**), and ventral (**l**) view. **m–o** *W. tendringensis*, gen. et sp. nov. (NMS.Z.2021.40.134), omal extremity of right coracoid in dorsal (**m**), medial (**n**), and ventral (**o**) view; the arrow denotes an enlarged detail. **p** *Phoeniculus purpureus* (SMF 6503), right coracoid in dorsal view. **q** *W. tendringensis*, gen. et sp. nov. (NMS.Z.2021.40.137), partial furcula. **r** furcula of *Ph. purpureus* (SMF 6503). **s**, **t** *W. tendringensis*, gen. et sp. nov. (NMS.Z.2021.40.134), distal end of right humerus in cranial (**s**) and caudal (**t**) view. **u** *Messelirrisor* sp. from the middle Eocene of Geiseltal (GMH L-9–1969) in cranial view. **v** *Messelirrisor halcyrostris* from Messel (SMF-ME 2245), right humerus in cranial view. **w** *Ph. purpureus* (SMF 7355), distal end of right humerus in cranial view. **x** *M. halcyrostris* (SMF-ME 10987a), distal end of right humerus and proximal end of right ulna. **y**, **z** *W. tendringensis*, gen. et sp. nov. (NMS.Z.2021.40.137), proximal end of left ulna in cranial (**y**) and caudal (**z**) view. **aa**, **bb** *Ph. purpureus* (SMF 7355), proximal end of left ulna in cranial (**aa**) and caudal (**bb**) view. **cc** *W. tendringensis*, gen. et sp. nov. (NMS.Z.2021.40.137), distal end of right ulna in ventral view. **dd** *Ph. purpureus* (SMF 7355), distal end of right ulna in ventral view. **ee**, **ff** *W. tendringensis*, gen. et sp. nov. (NMS.Z.2021.40.134), right carpometacarpus in dorsal (**ee**) and ventral (**ff**) view. **gg** *M. halcyrostris* from Messel (SMF-ME 10987a), left carpometacarpus in dorsal view. **hh**, **ii** *Phoeniculus purpureus* (SMF 6503), right carpometacarpus in dorsal (**hh**) and ventral (**ii**) view. **jj** *W. tendringensis*, gen. et sp. nov. (NMS.Z.2021.40.140), distal end of right tibiotarsus in cranial view. **kk–mm** *W. tendringensis*, gen. et sp. nov. (NMS.Z.2021.40.135), distal end of left tarsometatarsus in dorsal (**kk**), plantar (**ll**), and distal (**mm**) view. **nn–pp** *W. tendringensis*, gen. et sp. nov. (NMS.Z.2021.40.139), distal end of left tarsometatarsus in dorsal (**nn**), plantar (**oo**), and distal (**pp**) view. **qq** *M. grandis* (SMF-ME 10833), left tarsometatarsus in dorsal view. **rr–tt**, *Upupa epops* (SMF 19549), distal end of left tarsometatarsus in dorsal (**rr**), plantar (**ss**), and distal (**tt**) view. *apf* apophysis furculae, *cdd* condylus dorsalis, *cdv* condylus ventralis, *ctd* cotyla dorsalis, *ctv* cotyla ventralis, *epd* epicondylus dorsalis, *flx* processus flexorius, *fmb* fossa musculi brachialis, *icl* incisura lateralis, *icm* incisura medialis, *ldc* attachment site of ligamentum dorsale cubiti, *llc* attachment site of ligamentum limitans cubiti, *mpr* medial projection of extremitas sternalis of coracoid, *mps* attachment site of musculus pronator superficialis, *olc* olecranon, *pim* processus intermetacarpalis, *pra* processus retroarticularis, *prj* projection of facies articularis clavicularis, *tbc* tuberculum ventrale, *tsd* tuberculum supracondylare dorsale, *tsv* tuberculum supracondylare ventrale. The scale bars equal 5 mm

shed light on the poorly known *Laputavis robusta* from Walton-on-the-Naze, which – on the basis of fragmentary material – was initially described as an apodiform bird (Dyke 2001a, b). Two further fossils show affinities to the North American "*Neanis*" *kistneri* and may be stem group representatives of the Piciformes.

Material and methods

The examined fossil specimens are deposited in the Geiseltalsammlung, Martin-Luther Universität of Halle-Wittenberg, Germany (GMH); the Geological Museum of the University of Copenhagen, Denmark (MGUH); the Royal Belgian Institute of Natural Sciences, Brussels, Belgium (IRSNB); the Natural History Museum, London, UK (NHMUK); the National Museums Scotland, Edinburgh, UK (NMS); and the Senckenberg Research Institute Frankfurt, Germany (SMF).

Most specimens described below are represented by multiple skeletal elements of the same individual, which were found in association and are catalogued under the same number. Red dots on some of the fossil bones were added by the collector, M. Daniels, in order to prevent a mix-up of elements of different individuals.

Systematic palaeontology

Aves Linnaeus, 1758
Picocoraciades sensu Sangster et al. (2022)
Bucerotes Fürbringer, 1888
Upupiformes (Seebohm, 1890)
Waltonirrisor, gen. nov.

Type species. Waltonirrisor tendringensis, sp. nov.

Differential diagnosis. Differs from *Messelirrisor* Mayr, 1998 in that the processus flexorius of the humerus is strongly distally protruding; the proximal end of the ulna lacks a marked dorsal embossment at the attachment of ligamentum dorsale cubiti; the tarsometatarsus has a wide incisura intertrochlearis lateralis.

Etymology. The taxon name is derived from the name of the type locality and *Irrisor*, an old name used for a taxon of wood hoopoes (Phoeniculidae).

Waltonirrisor tendringensis, sp. nov.

Holotype. NMS.Z.2021.40.134 (Fig. 1a; partial right coracoid, distal end of right humerus, partial right radius, right carpometacarpus); collected in 1990 by M. Daniels (original collector's number WN 90655).

Diagnosis. As for genus.

Etymology. The species epithet refers to the Tendring district in the county of Essex, to which Walton-on-the-Naze belongs.

Type locality and horizon. Walton-on-the-Naze, Essex, United Kingdom; Walton Member of the London Clay Formation (previously Division A2; Jolley 1996; Rayner et al. 2009; Aldiss 2012), early Eocene (early Ypresian, 54.6−55 Ma; Collinson et al. 2016).

Referred specimens. NMS.Z.2021.40.135 (Fig. 1f; distal portion of left tarsometatarsus); collected in 1982 by M. Daniels (original collector's number WN 82401). NMS.Z.2021.40.136 (Fig. 1b; vertebra, distal end of left humerus, phalanx proximalis digiti majoris); collected in 1998 by M. Daniels (original collector's number WN 98982). NMS.Z.2021.40.137 (Fig. 1c; partial mandible, partial furcula, proximal ends of both ulnae, distal end of right ulna); collected in 1979 by M. Daniels (original collector's number WN 79240). NMS.Z.2021.40.138 (Fig. 1d; proximal end of right ulna); collected in 1982 by M. Daniels (original collector's number WN 82396). NMS.Z.2021.40.139 (Fig. 1g; distal portion of left tarsometatarsus); collected in 1994 by M. Daniels (original collector's number WN 94836B). NMS.Z.2021.40.140 (Fig. 1e; distal end of left tibiotarsus); collected in 1996 by M. Daniels (original collector's number WN 96968).

Measurements (maximum length, in mm). NMS.Z.2021.40.134: carpometacarpus, 9.4.

Remarks. NMS.Z.2021.40.134 and NMS.Z.2021.40.137 were figured by Mayr (1998: pl. 7). The fossils are of similar size to *Messelirrisor grandis*, which is the largest messelirrisorid known from Messel (other *Messelirrisor* species are distinctly smaller; Mayr 2006: tab. 1).

Description and comparisons. The mandible (NMS.Z.2021.40.137; Fig. 1h–l) exhibits a long, blade-like retroarticular process, which is a characteristic derived feature of the Upupidae and Phoeniculidae and enables foraging by gaping (Mayr 1998, 2000). The dorsal portion of this process is broken in the fossil, therefore impeding detailed comparisons with extant Upupiformes. The pars symphysialis is long and narrow.

As in extant Upupiformes (Fig. 1p), the coracoid (Fig. 1m–o) has a fairly wide and stout shaft. The facies articularis clavicularis forms a sternally directed projection (Fig. 1n), which gives the processus acrocoracoideus a markedly hook-shaped outline. The facies articularis scapularis is more concave than it is in extant Upupiformes. The tip of the processus procoracoideus is broken in NMS.Z.2021.40.134. The medial margin of the extremitas sternalis exhibits a small convexity, but unlike in the early Oligocene *Laurillardia* (Mayr et al. 2020) and crown group Upupiformes, it does not form a marked medial projection.

The furcula (Fig. 1q) features a small apophysis furculae, which is absent in extant Upupidae (Fig. 1r) and Phoeniculidae.

The distal end of the humerus (Fig. 1s, t) closely resembles the distinctive humerus of the Messelirrisoridae (Fig. 1u, v; Mayr 1998, 2000, 2020). Ventroproximal to the tuberculum supracondylare ventrale there is a marked attachment site for musculus pronator superficialis. The tuberculum supracondylare dorsale is small but well-defined and the epicondylus dorsalis forms a dorsally directed projection. The fossa musculi brachialis is extensive but shallow and located near the medial margin of the bone. The elongated condylus ventralis bears a shallow fossa on its cranial surface. The processus flexorius is strongly developed and protrudes markedly distally; with regard to its development it corresponds to the flexor process of a humerus from the middle Eocene of Geiseltal (Fig. 1u), whereas the processus flexorius is less pronounced in at least some of the *Messelirrisor* specimens from Messel, in an unnamed upupiform bird from the early Oligocene of Belgium reported by Mayr and Smith (2013), and in crown group Upupiformes.

The olecranon of the ulna (Fig. 1y, z) is fairly long but shorter than in crown group Upupiformes. Distal to the processus cotylaris dorsalis there are two longitudinal muscular attachment scars, presumably for ligamentum limitans cubiti and ligamentum dorsale cubiti (sensu Watanabe et al. 2021; Fig. 1z). The attachment site for the latter ligament forms a marked dorsal embossment in *Messelirrisor* (Fig. 1x) and crown group Upupiformes (Fig. 1aa, bb). The distal end of the bone is characterised by a proximodistally long condylus dorsalis, a craniocaudally extensive condylus ventralis, and a large and cranially projected tuberculum carpale.

The carpometacarpus (Fig. 1ee, ff) corresponds well to that of messelirrisorids (Fig. 1gg). The extremitas proximalis is proportionally larger than in crown group Upupiformes (Fig. 1hh, ii). Unlike in the latter, but as in other early Cenozoic stem group Upupiformes, there is a small processus intermetacarpalis at the proximal end of the os metacarpale majus. This process serves for the attachment of musculus extensor carpi ulnaris, which − despite its name − flexes the hand section of the wing and was secondarily lost in the lineage leading to hoopoes and wood hoopoes, in which an improved leverage of this muscle appears to no longer have been needed (see Stegmann 1965, who used the old name m. flexor metacarpi ulnaris for this muscle, which actually belongs to the extensor group found in non-avian tetrapods George and Berger 1966). As in crown group Upupiformes, the os metacarpale minus has undulated margins.

The distal tibiotarsus (Fig. 1jj) resembles that of extant Upupidae. The condyli are of subequal size.

The tarsometatarsi (Fig. 1kk−pp) are referred to *Waltonirrisor* based on their very small size and upupiform-like morphology. The foramen vasculare distale is very large.

As in crown group Upupiformes, the trochlea metatarsi II is large and reaches far distally (in NMS.Z.2021.40.135 the medial portion of the trochlea metatarsi II is damaged). Unlike in *Messelirrisor* (Fig. 1qq) and extant Upupidae (Fig. 1rr–tt) the incisura lateralis is very wide; this incision is also wide in the Phoeniculidae, in which the trochlea metatarsi IV is very narrow.

Coraciiformes Forbes, 1884
Coracii Wetmore and Miller, 1926
cf. **Primobucconidae** Feduccia and Martin, 1976
Laputavis Dyke, 2001

Taxonomic remarks. The holotype of *Laputavis robusta* (Dyke 2001a) consists of associated fragmentary bones from Walton-on-the-Naze, including partial coracoids, a partial humerus, and a partial tarsometatarsus (Fig. 2a). The species was initially described as "*Laputa robusta*" by Dyke (2001a), which was later corrected to *Laputavis robusta*, because the taxon name *Laputavis* was preoccupied (Dyke 2001b). In the original description, *L. robusta* was considered to be an apodiform bird, but this classification was poorly founded (Mayr 2001), and Mayr (2009: 130) noted resemblances to the Coraciiformes. We identified two specimens in the Daniels collection that corroborate coraciiform affinities of *L. robusta*. These two fossils agree with the *Laputavis robusta* holotype and differ from the specimens we refer to *Septencoracias* in the shape of the processus acrocoracoideus of the coracoid, which has a less hook-shaped outline and a more medially directed tip (Fig. 2).

Laputavis robusta (Dyke, 2001)

Referred specimens. NMS.Z.2021.40.141 (Fig. 2b; two cervical vertebrae, extremitas omalis of right coracoid, fragmentary proximal portion of right humerus, distal portion of right carpometacarpus); collected in 1986 by M. Daniels (original collector's number WN 86541A). NMS.Z.2021.40.142 (Fig. 2c; partial left coracoid, extremitates craniales of both scapulae, furcula, distal end of right humerus); collected in 1987 by M. Daniels (original collector's number WN 87576).

Locality and horizon. Walton-on-the-Naze, Essex, United Kingdom; Walton Member of the London Clay Formation (previously Division A2; Jolley 1996; Rayner et al. 2009; Aldiss 2012), early Eocene (early Ypresian).

Description and comparisons. The coracoids of NMS.Z.2021.40.141 and NMS.Z.2021.40.142 closely resemble that of the *L. robusta* holotype in the shape of the processus acrocoracoideus, which exhibits pneumatic openings in its dorsal surface and – unlike in the *Septencoracias* fossils described below (Fig. 2e) – is only weakly hooked and has a medially rather than sternally directed tip (Fig. 2a–c). Specimens NMS.Z.2021.40.141 and NMS.Z.2021.40.142 exhibit a tiny foramen in the coracoid,

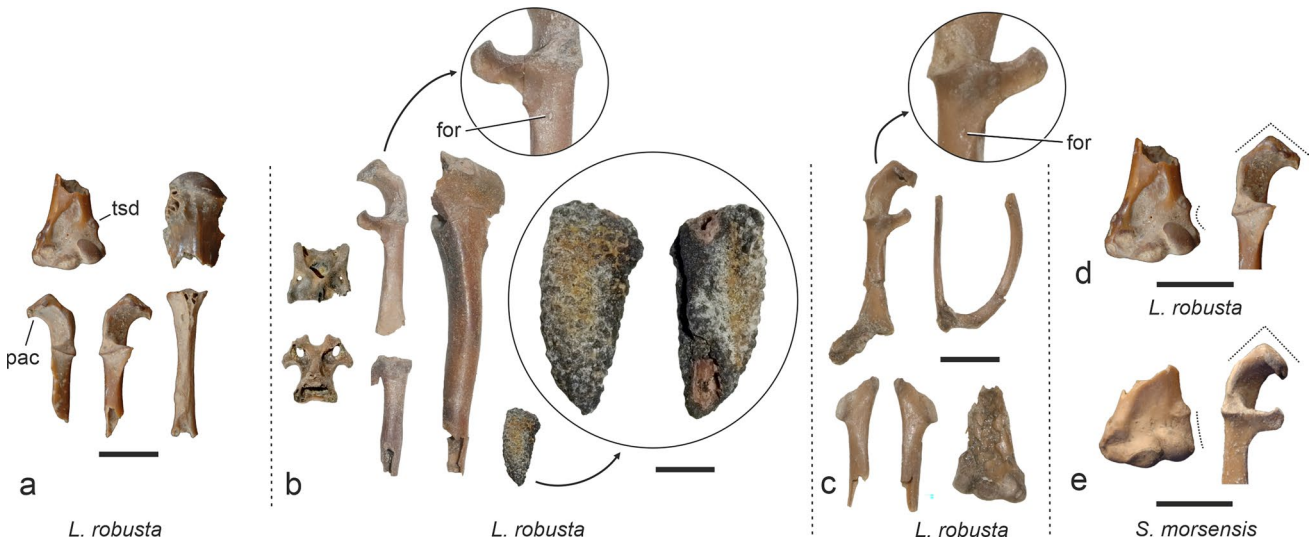

Fig. 2 Fossils of *Laputavis robusta* and *Septencoracias morsensis* from Walton-on-the-Naze. **a** the holotype of *L. robusta* (NHMUK A 6206). **b** *L. robusta*, referred specimen NMS.Z.2021.40.141. **c** *L. robusta*, referred specimen NMS.Z.2021.40.142. **d**, **e** comparison of the distal humerus and omal extremity of the coracoid of the *L. robusta* holotype (**d**) with a specimen we refer to *S. morsensis* (**e**: NMS.Z.2021.40.143); the dotted lines indicate differences in the shape of the processus acrocoracoideus of the coracoid and the dorsal margin of the distal humerus. The arrows in **b** and **c** denote enlarged details of the coracoid; the lower arrow in **b** indicates details of the tuberculate encrustations (possible remnants of toe pads) around a pedal phalanx of NMS.Z.2021.40.141 in two views. *for* foramen, *pac* processus acrocoracoideus, *tsd* tuberculum supracondylare dorsale. The scale bars equal 5 mm

sternal to the facies articularis scapularis, which may either be a rudimentary foramen nervi supracoracoidei or – perhaps more likely – a pneumatic or nutrient foramen.

The dorsal margin of the distal end of the humerus is markedly convex and exhibits a small but well-defined tuberculum supracondylare dorsale. As far as comparisons are possible, the tarsometatarsus corresponds to that of the *Septencoracias* fossils described below.

NMS.Z.2021.40.141 includes a pedal phalanx that is embedded in a concretion with a tuberculate surface (Fig. 2b). Similar encrustations are known from other birds from Walton-on-the-Naze (Mayr and Kitchener 2023a: fig. 13ff, 2023b: fig. 8a) and were interpreted as remnants of the keratinised toe pads by the collector, M. Daniels.

Septencoracias Bourdon et al., 2016

Taxonomic remarks. The fossils described in the following closely resemble the holotype of *Septencoracias morsensis* from the Danish Fur Formation, which was described by Bourdon et al. (2016). Characteristic shared derived features include a medially-bent distal end of the first phalanx of the second toe and lateral bulges on the distal ends of the first and second phalanges of the third toe.

The material from Walton-on-the-Naze includes at least two very similar *Septencoracias*-like species, which can be clearly distinguished in the morphologies of the coracoid, furcula, and carpometacarpus. One of these species differs from *S. morsensis* in some features, while the assignment of the other species to *S. morsensis* is largely by default.

Septencoracias morsensis has not been compared with *Laputavis robusta* by Bourdon et al. (2016), and we note that the *S. morsensis* holotype cannot be differentiated from the *L. robusta* holotype, because the coracoid is not preserved in the *S. morsensis* holotype and the humerus and tarsometatarsus allow only very limited comparisons with the similar-sized fragmentary humerus and tarsometatarsus of the *L. robusta* holotype. The new fossils from Walton-on-the-Naze that we assign to *S. morsensis* differ from the *Laputavis robusta* holotype in that the dorsal margin of the distal humerus is straight rather than distinctly concave (Fig. 2d, e). Given the strong overall similarity of the *Laputavis* and *Septencoracias* fossils and the coeval ages and geographical proximity of the Fur Formation (the type locality of *S. morsensis*) and Walton-on-the-Naze (the type locality of *L. robusta*), we consider it possible that *Septencoracias* Bourdon et al., 2016 is a junior synonym of *Laputavis* Dyke, 2001. However and as detailed above, this hypothesis cannot be substantiated or disproven with the currently available fossil material. Regardless of a possible synonymy of the taxa *Septencoracias* and *Laputavis*, the two species from Walton-on-the-Naze that we assign to *Septencoracias* and describe below are distinguished from the specimens we refer to *Laputavis robusta*.

Septencoracias morsensis Bourdon et al., 2016

Referred specimens. NMS.Z.2021.40.143 (Fig. 3a; partial skeleton including partial mandibular ramus, partial quadrates, several vertebrae, both coracoids, left scapula, furcula, sternum, proximal and distal ends of right humerus, distal end of left humerus, left ulna, both carpometacarpi, both phalanges proximales digitorum majores, left femur, distal end of right tibiotarsus, incomplete left tarsometatarsus, distal end of right tarsometatarsus, pedal phalanges); collected in 1980 by M. Daniels (original collector's number WN 80285). NMS.Z.2021.40.144 (Fig. 3b; partial skeleton including both quadrates, several vertebrae, right coracoid, extremitas omalis of left coracoid, right scapula, distal end of right humerus, proximal portion of right ulna, partial left radius, left carpometacarpus, right phalanx proximalis digiti majoris, distal portion of right tibiotarsus); collected in 1987 by M. Daniels (original collector's number WN 87555). NMS.Z.2021.40.145 (not figured; vertebra, left coracoid, extremitas cranialis of left scapula, fragment of furcula, proximal end of left carpometacarpus); collected in 2002 by M. Daniels (original collector's number WN 021048B). SMF Av 655 (figured by Mayr 2022b; partial skeleton including large portions of the mandible, the left jugal arch, left quadrate, nine vertebrae or fragments thereof, right carpometacarpus, distal section of right radius, nearly complete right tibiotarsus, distal section of left tibiotarsus, right fibula, fragment of left trochlea metatarsi IV, and most pedal phalanges of the left foot).

Locality and horizon. Walton-on-the-Naze, Essex, United Kingdom; Walton Member of the London Clay Formation (previously Division A2; Jolley 1996; Rayner et al. 2009; Aldiss 2012), early Eocene (early Ypresian).

Measurements (maximum lengths, in mm). NMS.Z.2021.40.143: right coracoid, 20.1; left coracoid, 19.8; left ulna, 37.8 [37.8]; right carpometacarpus, 18.9; left carpometacarpus, 19.0 [17.6]; left femur, 20.7 [20.5]; tarsometatarsus, length as preserved, 14.0; estimated total length, ~ 15.4 [15.5]. NMS.Z.2021.40.144: right coracoid, 20.0; left carpometacarpus, 17.4. Values in brackets indicate the dimensions of the holotype of *Septencoracias morsensis* (after Bourdon et al. 2016).

Description and comparisons. A partial ramus mandibulae and both quadrates are preserved in NMS.Z.2021.40.143 (Figs. 3a, 4g, h). The quadrates are also present in NMS.Z.2021.40.144 (Fig. 4e, f), and the bone closely resembles a quadrate from Walton-on-the-Naze (Fig. 4i), which was referred to *Septencoracias morsensis* and described by

Fig. 3 Fossils of *Septencoracias* spp. and undetermined Coracii from Walton-on-the-Naze. **a**, **b** specimens referred to *Septencoracias morsensis* (**a**: NMS.Z.2021.40.143, **b**: NMS.Z.2021.40.144). **c**, **d** *S. simillimus*, sp. nov. (**c**: holotype, NMS.Z.2021.40.146, **d**: NMS.Z.2021.40.147). **e, f** Coracii, gen. et sp. indet. (**e**: NMS.Z.2021.40.150, **f**: NMS.Z.2021.40.152). *pyg* pygostyle, *ste* sternum. The scale bars equal 5 mm

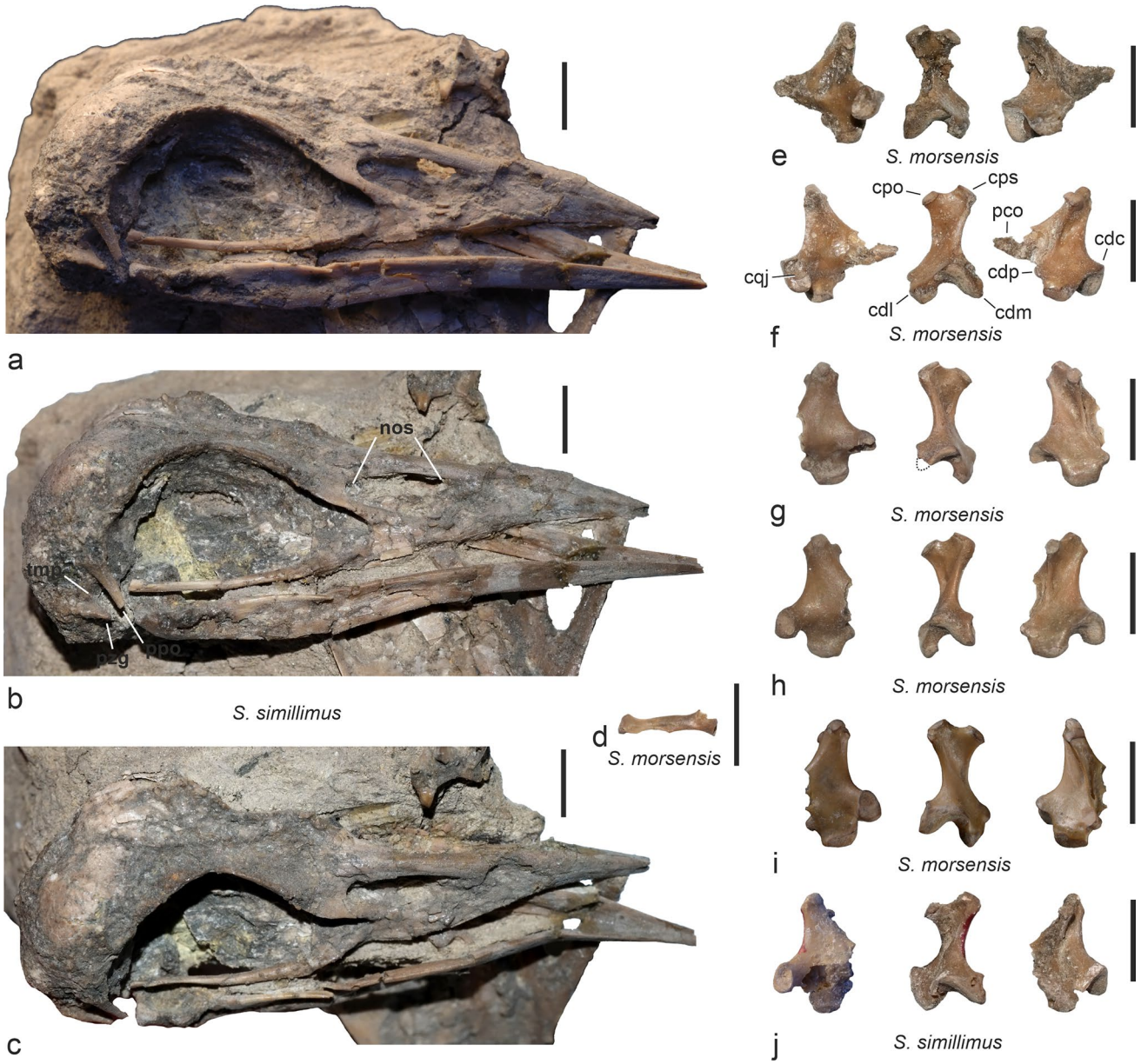

Fig. 4 Skull (**a–c**), pterygoid (**d**), and quadrates (**e–j**) of *Septencoracias* spp. from Walton-on-the-Naze. **a–c** *Septencoracias simillimus*, sp. nov. (holotype, NMS.Z.2021.40.146), skull in lateral (**a**, **b**) and dorsolateral (**c**) view. **d** *S. morsensis* (NMS.Z.2021.40.143), pterygoid. **e**, **f** *S. morsensis* (NMS.Z.2021.40.144), left (**e**) and right (**f**) quadrate in lateral, caudal, and medial view. **g**, **h** *S. morsensis* (NMS.Z.2021.40.143), left (**g**) and right (**h**) quadrate in lateral, caudal, and medial view; the dotted line in **g** indicates the reconstructed shape of the condylus lateralis. **i** *S. morsensis* (SMF Av 655), left quadrate in lateral, caudal, and medial view. **j** *S. simillimus*, sp. nov. (holotype, NMS.Z.2021.40.146), right quadrate in lateral, caudal, and medial view. *cdc* condylus caudalis, *cdl* condylus lateralis, *cdm* condylus medialis, *cdp* condylus pterygoideus, *cpo* capitulum oticum, *cps* capitulum squamosum, *cqj* cotyla quadratojugalis, *nos* nostril, *pco* processus orbitalis, *ppo* processus postorbitalis, *pzg* processus zygomaticus, *tmp* fossa temporalis. The scale bars equal 5 mm

Mayr (2022b). As in the latter specimen, there is an embossment ventral to the cotyla quadratojugalis and a tuberculum subcapitulare distal to the capitulum squamosum. The quadrates of NMS.Z.2021.40.144 preserve the processus orbitalis, which is missing in the specimen described by Mayr (2022b). The pterygoid (NMS.Z.2021.40.143; Fig. 4d) lacks a facies articularis basipterygoidea.

NMS.Z.2021.40.144 and NMS.Z.2021.40.143 include several vertebrae. The atlas (NMS.Z.2021.40.143; Fig. 5g, h) has a dorsally open incisura fossae. The third cervical vertebra (NMS.Z.2021.40.144; Fig. 5i) bears small lateral foramina and resembles the corresponding vertebra of *Coracias* (Coraciidae; Fig. 5j). The pygostyle (NMS.Z.2021.40.143;

Fig. 3a) is of similar size and shape to that of the *S. morsensis* holotype.

The coracoid (Fig. 6g–j) resembles that of the *Laputavis robusta* holotype (Fig. 6a–d), but the processus acrocoracoideus has a somewhat more hooked shape with a less medially projected tip. Unlike in the new *Septencoracias* species described below (Fig. 6k–n), the well-developed processus procoracoideus projects perpendicular to the longitudinal axis of the bone. The processus acrocoracoideus exhibits pneumatic openings in its dorsal surface. There is a notch in the medial side of the extremitas sternalis (Figs. 5k, 6h), which is very weakly developed or absent in extant Coracii (Fig. 5m, n), but occurs in, e.g., the Trogoniformes, Meropidae, Alcedinidae, and some piciform birds. The coracoid is not preserved in the *S. morsensis* holotype.

The furcula (Fig. 5o) is broadly U-shaped and lacks an apophysis furculae. The extremitas omalis is caudally kinked and tapers to a pointed tip; it is narrower than in extant rollers and, unlike in the Meropidae and Alcedinidae (Höfling and Alvarenga 2001: fig. 2), there is no processus acrocoracoideus. The furcula is not preserved in the *S. morsensis* holotype.

The scapula of NMS.Z.2021.40.143 (Fig. 3a) has a sharply curved caudal end. However, the tip of the bone is broken and was reattached by the collector, so that this curvature may be more pronounced than it actually was.

The sternum is not preserved in the *S. morsensis* holotype. In NMS.Z.2021.40.143 much of the bone is present (Fig. 5y) and shows the morphology characteristic for the Coracii, with two pairs of deep incisions in the caudal margin. The spina externa is broken.

Only fragments of the proximal and distal ends of the humerus are preserved in the specimens. The fossa pneumotricipitalis exhibits a large pneumatic opening. The distal end of the bone (Fig. 6q, r) corresponds to the distal humerus of the *L. robusta* holotype (Fig. 6o, p) in size, but the dorsal margin is straight and not markedly concave as it is in *L. robusta*.

The ulna (Fig. 3a, b) is stouter than that of extant Coracii and the cotyla dorsalis reaches farther distally.

The carpometacarpus (Fig. 5ee) agrees with that of the roller fossil from Walton-on-the-Naze described by Mayr (2022b). Like in the latter fossil, the new specimens exhibit a weakly developed processus intermetacarpalis. Distally, the os metacarpale minus does not project beyond the os metacarpale majus. The proximal end of the os metacarpale minus bears a small, ventrally directed, and tubercle-like projection. The very narrow spatium intermetacarpale of NMS.Z.2021.40.144 (Fig. 3b) is likely to be an artefact of preservation.

The phalanx proximalis digiti majoris (Fig. 3a) exhibits a weakly developed processus internus indicis.

The femur (Fig. 3a) has similar proportions to that of the Brachypteraciidae (the femur of the Coraciidae is somewhat stouter).

The distal tibiotarsus of NMS.Z.2021.40.144 (Fig. 3b) corresponds to the distal tibiotarsus of the roller fossil described by Mayr (2022b) except for the somewhat less pronounced lateral tuberositas retinaculi extensori. Unlike in the late Eocene *Geranopterus* (Mayr and Mourer-Chauviré 2000: fig. 8T) and extant Coracii (Mayr 2022b: fig. 4v, w), the sulcus extensorius is medially situated, whereas it is centrally located in *Geranopterus* and extant rollers.

The tarsometatarsus is not completely preserved, but the bone can be restored by digitally superimposing the partial left tarsometatarsus and the distal portion of the right tarsometatarsus of NMS.Z.2021.40.143 (Fig. 6gg). In its morphology it closely resembles the tarsometatarsus of the *S. morsensis* holotype (Fig. 6hh). The hypotarsus corresponds to that of extant Coracii in that there is a single canal, presumably for the tendon of musculus flexor digitorum longus. As in the *L. robusta* holotype, the medial foramen vasculare proximale is much larger than the lateral one. In accordance with the long hallux of the fossil species, the fossa metatarsi I is large. On the distal end of the bone, the canalis interosseus distalis is plantarly open, which is a derived feature of the Coracii (Mayr et al. 2004).

As in the holotype of *Septencoracias morsensis*, the first phalanx of the hallux is the longest pedal phalanx (Fig. 6xx), whereas this phalanx is of subequal length to the first phalanx of the third toes in *Primobucco mcgrewi*. The distal end of the first phalanx of the fourth toe is bent medially and exhibits a lateral protuberance, as it does in the holotype of *S. morsensis* and the roller specimen described by Mayr (2022b; note that the phalanx identified as the first phalanx of the fourth toe in this study is likely to be the second phalanx).

Septencoracias simillimus, sp. nov.

Holotype. NMS.Z.2021.40.146 (Fig. 3c; partial skeleton including skull, partial right quadrate, several vertebrae, right coracoid, both scapulae, furcula, sternum, right humerus, left humerus lacking proximal end, right ulna, proximal portion of left ulna, right radius, distal end of left radius, left carpometacarpus, proximal portion of right carpometacarpus, both phalanges proximales digitorum majores, proximal and distal ends of right femur, right tibiotarsus, right tarsometatarsus, several pedal phalanges); collected in 1983 by M. Daniels (original collector's number WN 83456).

Differential diagnosis. Differs from the *Laputavis robusta* holotype in that the processus acrocoracoideus of the coracoid has a more strongly hooked outline (Fig. 6b, k).

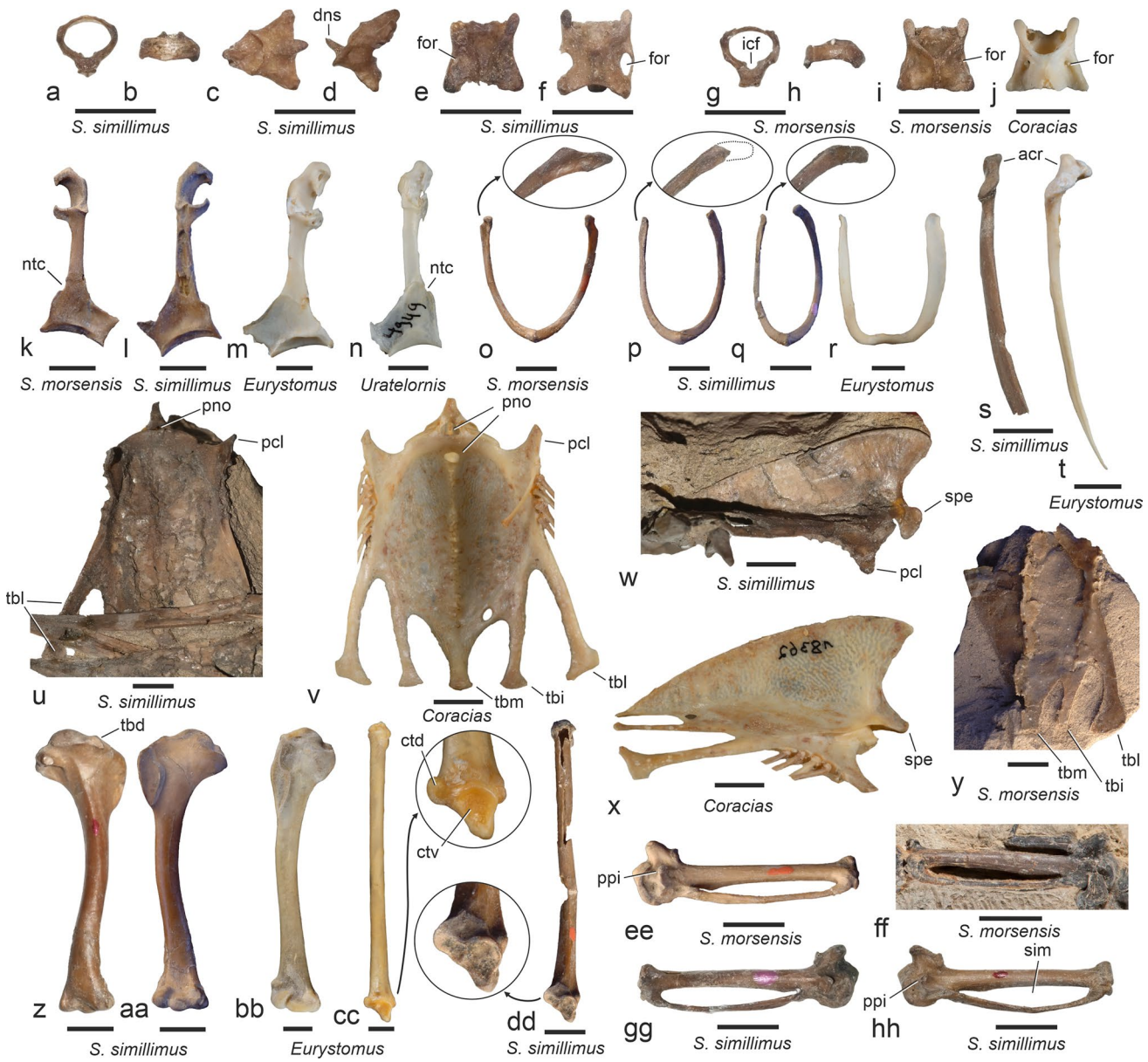

Distinguished from the holotype of *Septencoracias morsensis* in that the carpometacarpus has a wider spatium intermetacarpale (Fig. 5ff–hh); the proximal end of the tarsometatarsus is proportionally narrower (ratio of tarsometatarsus length to proximal width 4.5 versus 3.9 in the *S. morsensis* holotype). Differs from the newly identified fossils we refer to *S. morsensis* in that the processus procoracoideus of the coracoid points more towards the extremitas omalis (rather than pointing perpendicular to the longitudinal axis of the bone; Figs. 5k, l, 6g, k); the scapi clavicularum of the furcula are less widely spayed and the extremitas omalis does not taper to a point (Fig. 5o–r); the dorsal margin of the distal end of the humerus has a concave (rather than straight) outline (Fig. 6q, t).

Differs from the species of *Primobucco* in that the beak is proportionally longer (distinctly longer than the neurocranium, whereas it is shorter than the neurocranium in *Primobucco mcgrewi*); the processus postorbitalis is more robust; the first phalanx of the hallux is proportionally longer (longer than all other pedal phalanges, whereas it is of subequal length to the first phalanx of the third toe in *P. mcgrewi*).

The new species is distinctly smaller than the species of *Paracoracias* and *Eocoracias* (humerus length 32.1 mm versus 44.4–45.7 mm in *E. brachyptera* and 43.6 mm in *P. occidentalis*), from which it also differs in that the tibiotarsus is slenderer and proportionally longer (subequal to humerus in length, whereas it is distinctly shorter than the humerus in *Eocoracias* and *Paracoracias*).

◂**Fig. 5** Selected bones of *Septencoracias* spp. from Walton-on-the-Naze in comparison to extant rollers. **a**, **b** atlas of *Septencoracias simillimus*, sp. nov. (holotype, NMS.Z.2021.40.146) in caudal (**a**) and dorsal (**b**) view. **c**, **d** axis of *S. simillimus*, sp. nov. (holotype, NMS.Z.2021.40.146) in dorsal (**c**) and lateral (**d**) view. **e** third cervical vertebra (dorsal view) of *S. simillimus*, sp. nov. (holotype, NMS.Z.2021.40.146). **f** fourth cervical vertebra (dorsal view) of *S. simillimus*, sp. nov. (holotype, NMS.Z.2021.40.146). **g**, **h** atlas of *S. morsensis* (NMS.Z.2021.40.143) in caudal (**g**) and laterodorsal (**h**) view. **i** third cervical vertebra (dorsal view) of *S. morsensis* (NMS.Z.2021.40.144). **j** third cervical vertebra (dorsal view) of *Coracias garrulus* (SMF 1618) in dorsal view. **k** *S. morsensis* (NMS.Z.2021.40.144), right coracoid in dorsal view. **l** *S. simillimus*, sp. nov. (NMS.Z.2021.40.147), left coracoid in dorsal view. **m** *Eurystomus glaucurus* (SMF 518), left coracoid in dorsal view. **n** *Uratelornis chimaera* (SMF 4949), left coracoid in dorsal view. **o** *S. morsensis* (NMS.Z.2021.40.143), furcula; the arrow denotes a detail of the extremitas omalis. **p**, **q** *S. simillimus*, sp. nov. (**p**: holotype, NMS.Z.2021.40.146, **q**: NMS.Z.2021.40.147), furcula; the arrows denote details of the extremitas omalis, the dotted line in **p** indicates the reconstructed shape of the missing tip. **r** *E. glaucurus* (SMF 518), furcula. **s** *S. simillimus*, sp. nov. (holotype, NMS.Z.2021.40.146), scapula in ventral view. **t** *E. glaucurus* (SMF 518), scapula in ventral view. **u**, **w** *S. simillimus*, sp. nov. (holotype, NMS.Z.2021.40.146), sternum in dorsal (**u**) and lateral (**w**) view. **v**, **x** *Coracias caudatus* (SMF 18362), sternum in dorsal (**v**) and lateral (**x**) view; the image in **x** shows the mirrored left side of the bone. **y** *S. morsensis* (NMS.Z.2021.40.143), sternum in ventral view. **z**, **aa** *S. simillimus*, sp. nov. (holotype, NMS.Z.2021.40.146), right humerus in caudal (**z**) and cranial (**aa**) view. **bb** *E. glaucurus* (SMF 518), right humerus in cranial view. **cc** *E. glaucurus* (SMF 518), left ulna in cranial view; the arrow indicates and enlarged detail of the proximal end. **dd** *S. simillimus*, sp. nov. (NMS.Z.2021.40.143), left ulna in cranial view; the arrow indicates and enlarged detail of the proximal end. **ee** *S. morsensis* (NMS.Z.2021.40.143), left carpometacarpus in ventral view. **ff** right carpometacarpus (ventral view) of the holotype of *S. morsensis* (MGUH.VP 9509; from Bourdon et al. 2016, published under a Creative Commons Attribution 4.0 International License). **gg**, **hh** *S. simillimus*, sp. nov., right (**gg**) and left (**hh**) carpometacarpus in ventral view (**gg** NMS.Z.2021.40.147, **hh** holotype, NMS.Z.2021.40.146). *acr* acromion, *ctd* cotyla dorsalis, *ctv* cotyla ventralis, *dns* dens, *for* foramen, *icf* incisura fossae, *ntc* notch in medial margin of extremitas sternalis of coracoid, *pcl* processus craniolateralis, *pno* pneumatic opening, *ppi* processus pisiformis, *sim* spatium intermetacarpale, *spe* spina externa, *tbd* tuberculum dorsale, *tbi* trabecula intermedia, *tbl* trabecula lateralis, *tbm* trabecula mediana. The scale bars equal 5 mm

The tarsometatarsus is distinguished from that of the coraciiform-like *Microena goodwini* Harrison and Walker, 1977 from the London Clay of Bognor Regis, Sussex, UK (Fig. 6uu, vv), in that the shaft is proportionally narrower; the foramen vasculare distale is situated farther proximally; the trochlea metatarsi II reaches less far distally; and the plantar surface of the trochlea metatarsi III does not taper proximally.

Etymology. The species epithet is derived from simillimus (Lat.), alike, in reference to the great similarity to *Septencoracias morsensis*.

Type locality and horizon. Walton-on-the-Naze, Essex, United Kingdom; Walton Member of the London Clay Formation (previously Division A2; Jolley 1996; Rayner et al. 2009; Aldiss 2012), early Eocene (early Ypresian).

Referred specimens. NMS.Z.2021.40.147 (Fig. 3d; partial skeleton including left coracoid, extremitas sternalis of right coracoid, furcula, both scapulae lacking caudal ends, sternum, both humeri, left ulna, right radius, distal portion of left radius, right carpometacarpus, proximal portion of left carpometacarpus, both phalanges proximales digitorum majores); collected in 1982 by M. Daniels (original collector's number WN 82380). NMS.Z.2021.40.148 (partial skeleton including left coracoid, omal portion of right coracoid in piece of matrix, both scapulae, left humerus, distal end of right humerus, distal portion of left ulna, left radius lacking distal tip, left carpometacarpus, both phalanges proximales digitorum majores); collected in 1990 by M. Daniels (original collector's number WN 90645). NMS.Z.2021.40.149 (extremitas omalis of left coracoid, extremitates sternales of both coracoids, extremitas cranialis of right scapula, fragments of the furcula, distal end of left humerus); collected in 1991 by M. Daniels (original collector's number WN 91688).

Measurements (maximum length, in mm). NMS.Z.2021.40.146: right coracoid, 20.2; right humerus, 31.7 [31.6]; right ulna, 37.0 [37.8]; left carpometacarpus, 17.1 [17.6]; right tibiotarsus, length as preserved, 29.8 [30.9]; right tarsometatarsus, 14.6 [15.5]. NMS.Z.2021.40.147: left coracoid, 21.5; left humerus, 33.0; right humerus, 31.0; left ulna, 37.0; left radius, 35.2; right carpometacarpus, 18.4. NMS.Z.2021.40.148: left coracoid, 20.3, left humerus, 32.4, left carpometacarpus, 19.5. Values in brackets indicate the dimensions of the holotype of *Septencoracias morsensis* (after Bourdon et al. 2016).

Remarks. NMS.Z.2021.40.146 was figured by Mayr (1998: pl. 11) and was assigned to *Septencoracias* by Mayr (2022a: fig. 10.12e).

Description and comparisons. If not indicated otherwise, the description is mainly based on the largely complete specimen NMS.Z.2021.40.146. The skull of this fossil (Fig. 4a–c) is partially embedded in matrix, with most of the exposed surfaces of the neurocranium being poorly preserved. As in the *Septencoracias morsensis* holotype (Bourdon et al. 2016), it is large in relation to the body. The upper beak, the tip of which is missing, is distinctly longer than the neurocranium. The nostrils are large, a septum internasale appears to be absent. The caudal nasal bar is more inclined towards the longitudinal axis of the skull than in the distinctly larger unnamed roller from the London Clay of the Isle of Sheppey,

which was described by Mayr and Walsh (2018). A well-defined nasofrontal hinge is absent (this hinge is also absent in crown group Coracii, but occurs in the Momotidae, Todidae, Alcedinidae, and Meropidae). Lacrimals are not preserved, nor are articulation facets for these ossicles visible on the frontal bones. The interorbital section of the frontal bones has a similar width to that of extant Brachypteraciidae and is narrower than in the unnamed roller from the Isle of Sheppey. The processus postorbitalis is very long as it is in other rollers, but it is distinctly wider than the narrow postorbital

◂**Fig. 6** The coracoid (**a–n**), distal humerus (**o–w**), and tarsometatarsus (**x–ww**) of *Laputavis* and *Septencoracias* fossils from Walton-on-the-Naze. **a–d** extremitas omalis of the left (**a**, **c**) and right (**b**, **d**) coracoid of the holotype of *L. robusta* (NHMUK A 6206) in dorsal (**a**, **b**) and ventral (**c**, **d**) view. **e**, **f**, *L. robusta* (NMS.Z.2021.40.141), extremitas omalis of right coracoid in dorsal (**e**) and ventral (**f**) view. **g**, **h** left coracoid of *Septencoracias morsensis* (NMS.Z.2021.40.143) in dorsal (**g**) and ventral (**h**) view. **i**, **j** right coracoid of *S. morsensis* (NMS.Z.2021.40.144) in ventral (**i**) and dorsal (**j**) view. **k**, **l** left coracoid of *S. simillimus*, sp. nov. (NMS.Z.2021.40.147) in dorsal (**k**) and ventral (**l**) view. **m**, **n** right coracoid of *S. simillimus*, sp. nov. (holotype, NMS.Z.2021.40.146) in ventral (**m**) and dorsal (**n**) view. **o**, **p** distal end of the left humerus of the holotype of *L. robusta* (NHMUK A 6206) in cranial (**o**) and caudal (**p**) view. **q**, **r** distal end of the left (**q**) and right (**r**) humerus of *S. morsensis* (NMS.Z.2021.40.143) in cranial (**q**) and caudal (**r**) view. **s** distal end of the right humerus of *S. morsensis* (NMS.Z.2021.40.144) in cranial view. **t–v** distal end of the left (**t**) and right (**u**, **v**) humerus of *S. simillimus*, sp. nov. (holotype, NMS.Z.2021.40.146) in cranial (**t**, **u**) and caudal (**v**) view. **w** distal end of the right humerus of *S. simillimus*, sp. nov. (NMS.Z.2021.40.147) in caudal view. **x–z** partial right tarsometatarsus of the holotype of *L. robusta* (NHMUK A 6206) in dorsal (**x**), plantar (**y**), and proximal (**z**) view. **aa–ff** *S. morsensis* (NMS.Z.2021.40.143), partial left (**aa–cc**) and distal end of the right tarsometatarsus (**dd–ff**) in dorsal (**aa**, **dd**), plantar (**bb**, **ee**), proximal (**cc**), and distal (**ff**) view; the arrow denotes an enlarged detail. **gg** *S. morsensis*, reconstructed tarsometatarsus of NMS.Z.2021.40.143 by digitally superimposing the partial left tarsometatarsus and the mirrored distal portion of the right tarsometatarsus. **hh** left tarsometatarsus (dorsal view) of the holotype of *S. morsensis* (MGUH.VP 9509) with surrounding matrix digitally removed (surface scan, from Bourdon et al. 2016; published under a Creative Commons Attribution 4.0 International License). **ii–ll** *S. simillimus*, sp. nov. (holotype, NMS.Z.2021.40.146), right tarsometatarsus in dorsal (**ii**), plantar (**jj**), proximal (**kk**), and distal (**ll**) view. **mm–pp** Coracii, gen. et sp. indet. (NMS.Z.2021.40.150), right tarsometatarsus in dorsal (**mm**), plantar (**nn**), proximal (**oo**), and distal (**pp**) view. **qq–tt** Coracii, gen. et sp. indet. (NMS.Z.2021.40.152), left tarsometatarsus in dorsal (**qq**), plantar (**rr**), proximal (**ss**), and distal (**tt**) view. **uu**, **vv** *Microena goodwini*, holotype from Bognor Regis (Sussex, UK; NHMUK A 3685) in dorsal (**uu**) and plantar (**vv**) view. **ww** right tarsometatarsus (dorsal view) of an unidentified stem group representative of the Coracii from the early Eocene of Egem in Belgium (IRSNB Av 191; see Mayr and Smith 2019); the specimen was coated with ammonium chloride. **xx**, **yy** pedal phalanges of **xx** *S. morsensis* (NMS.Z.2021.40.143) and **yy** *S. simillimus*, sp. nov. (holotype, NMS.Z.2021.40.146); the toes are identified by Roman numerals. *cid* canalis interosseus distalis, *fdl* hypotarsal canal for tendon of musculus flexor digitorum longus, *mfv* medial foramen vasculare proximale, *ntc* notch in medial margin of extremitas sternalis, *pac* processus acrocoracoideus, *ppc* processus procoracoideus, *tsd* tuberculum supracondylare dorsale, *ttc* tuberositas musculi tibialis cranialis. The scale bars equal 5 mm

process of the Primobucconidae (Ksepka and Clarke 2010: fig. 3A) and the roller from the Isle of Sheppey. The processus zygomaticus is long, as in crown group Coracii and other coraciiform birds (e.g., Momotidae). The fossae temporales appear to have been shallow as in the *S. morsensis* holotype and the roller fossil from the Isle of Sheppey.

The quadrate (Fig. 4j) corresponds to that of the fossils we refer to *S. morsensis*.

The atlas (Fig. 5a, b; NMS.Z.2021.40.146) has a dorsally open incisura fossae and a craniocaudally wide arcus atlantis. The axis (Figs. 3c, 5c, d; NMS.Z.2021.40.146) resembles the axis of an undetermined stem group roller from the London Clay of the Isle of Sheppey (Mayr and Walsh 2018) and is craniocaudally longer than the axis of crown group Coracii (see Mayr and Walsh 2018: fig. 4); unlike in crown group Coracii, but as in the roller from the Isle of Sheppey, the processus spinosus is mediolaterally narrow. The third cervical vertebra (Fig. 5e; NMS.Z.2021.40.146) has a deeply incised craniodorsal margin of the corpus. The fourth cervical vertebra (Fig. 5f; NMS.Z.2021.40.146) exhibits a large lateral foramen; a similar foramen occurs in *Eurystomus* (Coraciidae), whereas the foramen is smaller in *Coracias* (Coraciidae) and *Uratelornis* (Brachypteraciidae), and absent in *Atelornis* (Brachypteraciidae) (Mayr and Walsh 2018: fig. 4).

The coracoid (Fig. 5l, 6k−n) resembles the coracoid of the specimens we refer to *S. morsensis*, but unlike in the latter the processus procoracoideus is inflected toward the processus acrocoracoideus. The medial portion of the processus acrocoracoideus of NMS.Z.2021.40.147 is wider in the sterno-omal direction than in the *L. robusta* holotype; in NMS.Z.2021.40.146 this part of the coracoid is damaged. As in the *S. morsensis* specimens, the medial margin of the extremitas sternalis forms a pronounced notch.

The extremitas omalis of the furcula is damaged in NMS.Z.2021.40.146 (Fig. 5p), but it is completely preserved in NMS.Z.2021.40.147 (Fig. 5q) and has a more broadly rounded and wider tip than that of the specimens we refer to *S. morsensis*. The scapi clavicularum are less widely splayed, the extremitas sternalis lacks an apophysis furculae.

Unlike in extant rollers, the acromion of the scapula is only weakly bifurcated (Fig. 5s, t).

The sternum and skull of NMS.Z.2021.40.146 are situated together in a piece of matrix (Figs. 3c, 5u, w). The left margo costalis exhibits six processus costales. Contrary to extant Coracii, the spina externa forms a marked dorsal bulge. As in extant rollers, there is a large, ventrally situated pneumatic foramen at the base of the spina externa. However, unlike in extant Coracii, a pneumatic opening in the cranial portion of the ventral surface of the corpus sterni is absent.

The humerus (Fig. 5z, aa) has a markedly sigmoidally curved shaft and agrees with the humeri of *Primobucco* in its proportions. As in the latter, the proximal end of the bone is much wider than it is in extant Coracii (Fig. 5bb). The tuberculum dorsale is larger than in extant rollers. The fossa pneumotricipitalis exhibits a large pneumatic opening. Unlike in NMS.Z.2021.40.143, a specimen we refer to *S. morsensis*, the dorsal margin of the distal end has a concave outline.

The carpometacarpus (Fig. 5gg, hh) has a wider spatium intermetacarpale than that of the *Septencoracias morsensis* holotype (Fig. 5ff). Unlike in extant Coraciidae and Brachypteraciidae, a well-developed processus intermetacarpalis is absent. There is a small, ventrally directed projection on the proximal end of the os metacarpale minus.

Only the proximal and distal ends of the femur are preserved in NMS.Z.2021.40.146 and these agree with the corresponding portions of the femur of the fossils we refer to *Septencoracias*.

The proximal end of the tibiotarsus of NMS.Z.2021.40.146 is damaged. The preserved portion of the bone corresponds to the tibiotarsus of a roller fossil from Walton-on-the-Naze described by Mayr (2022b).

The tarsometatarsus of the holotype (Fig. 6ii–ll) closely resembles that of the *Septencoracias morsensis* holotype (Fig. 6hh), but has a proportionally narrower proximal end (the ratio of the length of the tarsometatarsus to its proximal width is 4.5 versus 3.9 in the *S. morsensis* holotype). The tuberositas musculi tibialis cranialis is less pronounced than in the *L. robusta* holotype. The medial foramen vasculare proximale is much larger than the lateral one. The canalis interosseus distalis is plantarly open, which is a derived characteristic of the Coracii (Mayr et al. 2004). The hypotarsus (Fig. 6kk) corresponds to that of extant Coraciidae and exhibits a canal for the tendon of musculus flexor digitorum longus (Mayr 2016).

The phalanges (Fig. 6yy) correspond to those of the holotype of *S. morsensis* and the fossils of *S. morsensis* from Walton-on-the-Naze (NMS.Z.2021.40.143). As in the latter, the distal end of the first phalanx of the second toe is bent medially and bears a lateral protuberance. The second phalanx of the second toe of NMS.Z.2021.40.146 exhibits a widening in its midsection, which is likely to be of pathological origin.

Coracii, gen. et sp. indet.

Referred specimens. NMS.Z.2021.40.150 (Figs. 3e, 6mm–pp; proximal end of right femur, right tarsometatarsus, pedal phalanges); collected in 1983 by M. Daniels (original collector's number WN 83444). NMS.Z.2021.40.151 (distal end of left humerus); collected in 1980 by M. Daniels (original collector's number WN 80303A). NMS.Z.2021.40.152 (Fig. 3f, 6qq–tt; distal end of left tibiotarsus, left tarsometatarsus, some pedal phalanges); collected in 1997 by M. Daniels (original collector's number WN 97979). NMS.Z.2021.40.153 (various fragmentary bones including extremitates sternales of both coracoids, extremitas sternalis of the furcula, distal end of right humerus, proximal end of left ulna); collected in 1993 by M. Daniels (original collector's number WN 93808).

Locality and horizon. Walton-on-the-Naze, Essex, United Kingdom; Walton Member of the London Clay Formation (previously Division A2; Jolley 1996; Rayner et al. 2009; Aldiss 2012), early Eocene (early Ypresian).

Measurements (maximum length, in mm). NMS.Z.2021.40.150: right tarsometatarsus, 14.3. NMS.Z.2021.40.152: left tarsometatarsus, 15.0.

Remarks. These four specimens – which we do not assume to belong to the same species – are too incompletely preserved to be unambiguously assigned to one of the above species, which are very similar in size and morphology. NMS.Z.2021.40.150 possibly belongs to *Laputavis robusta*, and the tarsometatarsus of the specimen closely resembles that of the *L. robusta* holotype in size and morphology. The caput femoris of the femur of NMS.Z.2021.40.150 forms a proximal bulge, which is absent in the specimens we refer to *Septencoracias* and, unless it is a pathological feature, may represent an autapomorphy of *Laputavis*. The other bones are also likely to belong to one of the species described in the present study, but the preserved elements are not diagnostic enough for an unequivocal referral.

?***Primobucco*** Brodkorb, 1970
?***Primobucco*** sp.

Referred specimen. NMS.Z.2021.40.154 (Fig. 7a, d–g; distal end of left tibiotarsus, left tarsometatarsus, several pedal phalanges); collected in 1981 by M. Daniels (original collector's number WN 81371).

Tentatively referred specimens. NMS.Z.2021.40.155 (Fig. 7b; partial skeleton including both coracoid, extremitas cranialis of right scapula, sternum, partial right carpometacarpus, distal portion of left carpometacarpus, synsacrum, as well as other unprepared bones in small pieces of matrix); collected in 2002 by M. Daniels (original collector's number WN 021049). NMS.Z.2021.40.156 (Fig. 7c; partial skeleton including left coracoid, right coracoid lacking extremitas sternalis, left scapula, right scapula lacking caudal end, partial furcula, partial sternum, distal portions of both humeri, right ulna, right radius, left radius lacking proximal end, left carpometacarpus, carpal bones and wing phalanges); collected in 1988 by M. Daniels (original collector's number WN 88586).

Locality and horizon. Walton-on-the-Naze, Essex, United Kingdom; Walton Member of the London Clay Formation (previously Division A2; Jolley 1996; Rayner et al. 2009; Aldiss 2012), early Eocene (early Ypresian).

Measurements (maximum length, in mm). NMS.Z.2021.40.154: left tarsometatarsus, 13.3 [~13.1]. NMS.Z.2021.40.156: left coracoid, 15.7 [14.5–~16.5]; right radius, 25.2 [28.9–33.1];

Fig. 7 Fossils of a smaller, *Primobucco*-like stem group representative of the Coracii from Walton-on-the-Naze. **a** ?*Primobucco* sp., referred specimen NMS.Z.2021.40.154. **b** ?*Primobucco* sp., tentatively referred specimen NMS.Z.2021.40.155. **c** ?*Primobucco* sp., tentatively referred specimen NMS.Z.2021.40.156. **d–g** left tarsometatarsus of ?*Primobucco* sp. (NMS.Z.2021.40.154) in dorsal (**d**), plantar (**e**), proximal (**f**), and distal (**g**) view. **h** *Septencoracias simillimus*, sp. nov. (holotype, NMS.Z.2021.40.146), right tarsometatarsus in dorsal view. **i** cf. ?*Primobucco* sp. (NMS.Z.2021.40.156), left coracoid in dorsal view. **j** left coracoid of cf. *S. morsensis* (NMS.Z.2021.40.143) in dorsal view. **k** left os carpi radiale of the extant *Coracias garrulus* (Coraciidae) in cranial view. **l**, **m** left (**l**) and right (**m**) os carpi radiale of cf. ?*Primobucco* sp. (NMS.Z.2021.40.156) in cranial view. **n** cf. ?*Primobucco* sp. (NMS.Z.2021.40.156), sternum in lateral view. **o** *S. simillimus*, sp. nov. (holotype, NMS.Z.2021.40.146), sternum in lateral view. **p** cf. ?*Primobucco* sp. (NMS.Z.2021.40.156), distal end of left humerus in cranial view. **q** *S. simillimus*, sp. nov. (holotype, NMS.Z.2021.40.146), distal end of right humerus in cranial view. *cid* canalis interosseus distalis, *ela* sulcus for tendon of musculus extensor longus alulae, *mfv* medial foramen vasculare proximale, *mpr* medial projection, *spi* spina externa, *tbi* trabecula intermedia, *tbl* trabecula lateralis, *tbm* trabecula mediana, *tsd* tuberculum supracondylare dorsale. The scale bars equal 5 mm

Fig. 8 The taxon *Pristineanis*, gen. nov. from Walton-on-the-Naze. **a** the holotype of *Pristineanis minor*, gen. et sp. nov. (NMS.Z.2021.40.157). **b** sternum of the the holotype of *P. minor*, gen. et sp. nov. (NMS.Z.2021.40.157) in cranial view. **c** *Neanis schucherti* (uncatalogued cast of holotype in SMF), left coracoid in ventral view. **d** *P. minor*, gen. et sp. nov. (holotype, NMS.Z.2021.40.157), left coracoid in dorsal view. **e** *N. schucherti* (uncatalogued cast of holotype in SMF), left humerus in cranial view. **f**, **g** *P. minor*, gen. et sp. nov. (holotype, NMS.Z.2021.40.157), distal end of the right humerus in caudal (**f**) and cranial (**g**) view. **h–p** *P. minor*, gen. et sp. nov. (holotype, NMS.Z.2021.40.157), left (**h–l**) and right (**m–p**) tarsometatarsus in dorsal (**h**, **m**), dorsolateral (**i**), plantar (**j**, **n**), distal (**k**, **o**), and proximal (**l**, **p**) view. **q–s** *Pristineanis major*, gen. et sp. nov. (holotype, NMS.Z.2021.40.158), left tarsometatarsus in plantar (**q**), dorsal (**r**), and distal (**s**) view. *cmp* crista medianoplantaris, *fdl* hypotarsal canal for tendon of musculus flexor digitorum longus, *fhl* hypotarsal canal for tendon of musculus flexor hallucis longus, *flg* plantar flange formed by trochlea metatarsi IV, *fvd* foramen vasculare distale, *lfv* lateral foramen vasculare proximale, *mfv* medial foramen vasculare proximale, *spe* spina externa, *sul* sulcus on distal surface of trochlea metatarsi IV, *tsd* tuberculum supracondylare dorsale. The scale bars equal 5 mm

right ulna, 30.7 [30.8−34.7]; left carpometacarpus, 14.3 [14.0−15.8]. Values in brackets the dimensions of *Primobucco mcgrewi* (after Mayr et al. 2004 and Ksepka and Clarke 2010).

Remarks. The tarsometatarsus NMS.Z.2021.40.154 (Fig. 7d−g) can be unambiguously referred to the Coracii on the basis of a plantarly open canalis interosseus distalis. The bone is smaller than the tarsometatarsi we refer to *Septencoracias*, from which it also differs in a larger medial foramen vasculare proximale. NMS.Z.2021.40.154 corresponds in size to the tarsometatarsi of *Primobucco mcgrewi* and *P. perneri*, which measure ~ 13.1 and ~ 11.5−13.1 mm,

respectively (Mayr et al. 2004). The medial portion of the trochlea metatarsi IV is broken, so that this trochlea probably looks somewhat narrower than it originally was.

The coracoids of the tentatively referred specimens NMS.Z.2021.40.155 and NMS.Z.2021.40.156 (Fig. 7i) closely resemble those of the fossils we refer to *Septencoracias* (Fig. 7j), but they are distinctly smaller (in NMS.Z.2021.40.156 the length of the bone is 15.7 mm versus 19.8−20.3 mm in *S. morsensis* and *S. simillimus*, sp. nov.). The extremitas sternalis exhibits a distinct medial projection. The furcula also corresponds well to that of *Septencoracias*. However, the trabecula lateralis of the sternum (Fig. 7c) is narrower than in the fossils we refer to *Septencoracias*. Unlike in *Septencoracias* (Fig. 7o), the spina externa does not forms a marked dorsal bulge (Fig. 7n). The distal end of the humerus bears a small but well-defined tuberculum supracondylare dorsale (Fig. 7p). Apart from being smaller, the carpometacarpus corresponds well to the carpometacarpus of the fossils we refer to *Septencoracias*; the bone agrees with the carpometacarpus of *P. mcgrewi* in its length (see measurements above), whereas the carpometacarpi of *P. frugilegus* and *P. perneri* are larger (~15.0−~17.1 mm in *P. perneri* and 18.7 mm in *P. frugilegus* [Mayr et al. 2004]). The os carpi radiale (Fig. 7l, m) is narrower than the corresponding ossicle of extant Coracii (Fig. 7k) and lacks a sulcus for the tendon of musculus extensor longus alulae, the presence of which was identified as an apomorphy of the Picocoraciades by Mayr (2014). This sulcus is present in *Primobucco* specimens from Messel (Mayr 2014), which may challenge an assignment of NMS.Z.2021.40.156 to *Primobucco* and the Coracii.

?**Piciformes** (Meyer and Wolf, 1810)
Pristineanis, gen. nov.

Type species. Pristineanis minor, sp. nov.

Included species. Pristineanis kistneri (Feduccia, 1973).

Diagnosis. Characterised by a scapula with a long acromion; coracoid with long and slender processus procoracoideus; hypotarsus with two canals (for tendons of musculus flexor digitorum longus and musculus flexor hallucis longus); foramen vasculare distale very large; trochlea metatarsi IV forming a plantarly directed, wing-like flange.

Differential diagnosis. Differs from *Neanis* Brodkorb, 1965 in that the coracoid has a slenderer shaft and a less concave crista articularis sternalis; the distal humerus has a well-defined tuberculum supracondylare dorsale and a more protruding processus flexorius.

Distinguished from the zygodactyl Psittacopedidae in that the tarsometatarsus has a crista medianoplantaris.

Differs from the early Oligocene putative piciform *Picavus* Mayr and Gregorová, 2012 and the early Oligocene *Eocuculus* Chandler, 1999 in that the foramen vasculare distale of the tarsometatarsus is much larger.

Etymology. The taxon name is derived from pristinus (Lat.), former, and *Neanis*, in reference to the fact that the North American species we assign to this taxon was before known as *Neanis kistneri*.

Taxonomic remarks. The tarsometatarsus of *Pristineanis* closely resembles that of "*Neanis*" *kistneri* from the early Eocene Green River Formation. This species was described as a possible piciform bird by Feduccia (1973), who considered it to be related to *Neanis schucherti* (Fig. 8c, e), another fossil species from the Green River Formation described by Shufeldt (1913), which is the type species of the taxon *Neanis*. The holotype of "*N.*" *kistneri* is a badly crushed partial skeleton, but a second, more complete and better preserved specimen was reported by Weidig (2010), who likened the species to the piciform Galbulae. This new specimen shows "*N.*" *kistneri* to be distinguished from *N. schucherti* in a proportionally more elongate humerus, and here we assign the former species to the new taxon *Pristineanis,* as *P. kistneri*.

Pristineanis minor, sp. nov.

Holotype. NMS.Z.2021.40.157 (Fig. 8a; partial skeleton including both coracoids, cranial portions of both scapulae, caudal portion of ?right scapula, partial furcula, fragmentary cranial portion of sternum, distal end of right humerus, fragmentary distal portion of left humerus, distal portion of right ulna, distal portion of left tibiotarsus, both tarsometatarsi, several pedal phalanges); collected in 1984 by M. Daniels (original collector's number WN 84482B).

Differential diagnosis. Differs from *Pristineanis* ("*Neanis*") *kistneri* (Feduccia, 1973) in being slightly larger (tarsometatarsus length 12.2−12.3 mm versus 10.6−11.6 mm [Weidig 2010]). The new species is distinctly larger than *Neanis schucherti* Shufeldt, 1913 (length of coracoid 10.8 mm versus 15.6 mm [Feduccia 1976]).

Etymology. The species epithet refers to the fact that this is the smaller of the two *Pristineanis* species occurring at Walton-on-the-Naze.

Type locality and horizon. Walton-on-the-Naze, Essex, United Kingdom; Walton Member of the London Clay Formation (previously Division A2; Jolley 1996; Rayner et al. 2009; Aldiss 2012), early Eocene (early Ypresian).

Measurements (maximum length, in mm). Right coracoid, 15.6; left tarsometatarsus, 12.3; right tarsometatarsus, 12.2.

Description and comparisons. In size and morphology the coracoid resembles that of *Eotrogon stenorhynchus*, a recently described stem group trogon from Walton-on-the-Naze (Mayr et al. 2023). However, it differs from the latter species in that the facies articularis scapularis is shallower and the crista articularis sternalis more concave. As in *E. stenorhynchus*, the processus procoracoideus is narrow and its tip ventrally deflected.

The scapula has a very long acromion; the tuberculum coracoideum is small. The furcula appears to have been broadly U-shaped and lacks a well-developed apophysis furculae. The omal extremity is caudally kinked and has a broadly rounded tip.

As preserved, the corpus of the sternum is strongly vaulted. The spina externa is well-developed, mediolaterally narrow and has a truncate, unforked tip.

Only the distal end of the humerus is preserved. The bone shows a resemblance to the humerus of the above-described Coracii from Walton-on-the-Naze, but the processus flexorius is more strongly ventrally projecting. There is a well-delimited tuberculum supracondylare dorsale and the dorsal margin of the distal end has a concave outline.

The tibiotarsus likewise resembles that of the Coracii. The sulcus extensorius and pons supratendineus are medially situated. The condylus medialis is smaller than the condylus lateralis.

As far as comparisons are possible, the tarsometatarsus (Fig. 8h–p) agrees with that of *Pristineanis* ("*Neanis*") *kistneri* from the early Eocene North American Green River Formation (Weidig 2010: fig. 12; Grande 2013: fig. 132). The hypotarsus (Fig. 8l, p) has two canals, presumably for the tendons of musculus flexor digitorum longus and m. flexor hallucis longus (Mayr 2016). The foramina vascularia proximalia are small. There is a crista medianoplantaris in the proximal portion of the plantar surface of the shaft. The foramen vasculare distale is very large. The canalis interosseus distalis is plantarly open. The trochlea metatarsi II is plantarly deflected. The trochlea metatarsi IV forms a large, plantarly directed wing-like process (Fig. 8k, o), which indicates a semi-zygodactyl foot; this flange is also present in a specimen referred to *P. kistneri* (Mayr 2009: 200). In distal view the medial portion of the flange is separated by a weak furrow from the main portion of the trochlea metatarsi IV.

The pedal phalanges resemble those of the *Septencoracias* fossils in their proportions. As indicated by the length of its first phalanx, the hallux was well developed.

Pristineanis major, sp. nov.

Holotype. NMS.Z.2021.40.158 (Fig. 8q–s; partial left tarsometatarsus and pedal phalanx); collected in 1979 by M. Daniels (original collector's number WN 79253).

Differential diagnosis. The species differs from *P. minor* in its notably larger size.

Etymology. The species epithet refers to the fact that this is the larger of the two *Pristineanis* species occurring at Walton-on-the-Naze.

Type locality and horizon. Walton-on-the-Naze, Essex, United Kingdom; Walton Member of the London Clay Formation (previously Division A2; Jolley 1996; Rayner et al. 2009; Aldiss 2012), early Eocene (early Ypresian).

Measurements (in mm). Left tarsometatarsus, length as preserved, 13.4; estimated total length, ~ 14–15.

Remarks. This specimen is about ten percent larger than the tarsometatarsus of the *P. minor* holotype. Even though there are some sexually dimorphic extant bird species that show similar size differences, such a pronounced sexual dimorphism in size would be unusual among taxa of the Picocoraciades, and we consider it likely that the specimen belongs to a different species than *P. minor*. As in the latter species, the tarsometatarsus exhibits a plantarly open canalis interosseus distalis. Other features that can be seen in the specimen likewise correspond to those of *P. minor.*

Discussion

The early Eocene London Clay of Walton-on-the-Naze yielded stem group representatives of at least two of the three subclades of the Picocoraciades, with the Bucerotes being represented by small stem group Upupiformes and the Coraciiformes by four species of stem group Coracii. The affinities of *Pristineanis*, gen. nov. are more difficult to determine, but as detailed below the new taxon may be a representative of the Piciformes, the third major clade of the Picocoraciades.

The Messelirrisoridae are among the more abundant small perching birds in the avifauna of Messel in Germany (Mayr 2018), and small stem group Upupiformes also appear to have been common in Walton-on-the-Naze. *Waltonirrisor tendringensis*, gen. et sp. nov. was similar in size to *Messelirrisor grandis*, which is the largest species of the Messelirrisoridae (Mayr 2000). The morphology of the proximal end of the ulna, which lacks the dorsal embossment at the attachment site of ligamentum dorsale cubiti (sensu Watanabe et al. 2021) characteristic of *Messelirrisor* and crown group Upupiformes, suggests a position of *W. tendringensis* outside a clade formed by *Messelirrisor* and crown group Upupiformes. This phylogenetic placement also corresponds to the fact that the London Clay fossils are the earliest known representatives of the Upupiformes,

pre-dating the messelirrisorids from Messel by about seven million years. The similar morphology of the distal end of the humerus, which has a very long processus flexorius, suggests an assignment of the upupiform bird from Geiseltal (Fig. 1u) to the taxon *Waltonirrisor*.

Three equally-sized and morphologically very similar species of stem group rollers from Walton-on-the-Naze are assigned to *Laputavis robusta*, *Septencoracias morsensis* and *S. simillimus*, sp. nov. The two *Septencoracias* species share a medially kinked distal end of the first phalanx of the second toe. Unfortunately, pedal phalanges are unknown for *L. robusta*, but in size and morphology the bones preserved in the *L. robusta* fossils closely resemble those of the specimens we refer to *Septencoracias*. Actually, and as detailed above, *L. robusta* cannot be differentiated from *S. morsensis*, and there exists a possibility that the taxon *Septencoracias* Bourdon et al., 2016 is a junior synonym of *Laputavis* Dyke, 2001. The occurrence of three similar-sized and morphologically close species of stem group Coracii in Walton-on-the-Naze not only suggests that these species diverged only shortly before the strata of the London Clay were deposited, but also indicates that the species diversity of compression fossils from Lagerstätten-type fossil localities, such as Messel and the Green River Formation, may be significantly underestimated (a similar diversity of very similar species has recently been demonstrated for the Halcyornithidae from Walton-on-the-Naze; Mayr and Kitchener 2023c).

The new fossils exhibit two derived features of the Coracii, which are not visible in the *S. morsensis* and *L. robusta* holotypes, that is, very long processus postorbitales (skull) and a plantarly open canalis interosseus distalis of the tarsometatarsus. Plesiomorphic characteristics concern the shape of the processus acrocoracoideus of the coracoid (which is more elongated in crown group Coracii), the morphology of the acromion of the scapula (which is distinctly bifurcated in crown group Coracii), the much wider proximal end of the humerus, and the poorly developed processus intermetacarpalis of the carpometacarpus. The stem group rollers from Walton-on-the-Naze are here tentatively referred to the Primobucconidae, to which *Septencoracias* was also tentatively assigned by Bourdon et al. (2016). This placement is merely based on a similar overall morphology and most resemblances are likely to be plesiomorphic for the Coracii. However, we were unable to identify derived features unique to either *Primobucco* or *Septencoracias* and *Laputavis* that would unite any of these three taxa – to the exclusion of the others – with crown group Coracii.

The diversity of stem group representatives of the Coracii appears to have been high in the London Clay, and the fossils we assign to *Septencoracias* are clearly distinguished from the stem group roller from the Isle of Sheppey that was described by Mayr and Walsh (2018). Apart from being larger, this latter fossil has a much narrower processus postorbitalis and, as detailed by Mayr (2022b), its quadratum is distinguished from that of *Septencoracias*. The morphology of the *Laputavis* and *Septencoracias* tarsometatarsi corresponds well to that of a tarsometatarsus from Bognor Regis, Sussex, UK (Fig. 6uu, vv), which was described as *Microena goodwini* by Harrison and Walker (1977), who assigned the fossil to the Columbiformes (doves and pigeons). However, the *M. goodwini* tarsometatarsus is stouter than that of *Laputavis* and *Septencoracias,* and actually closely resembles a tarsometatarsus of an unidentified stem group roller from the early Eocene of Egem in Belgium (Fig. 6ww), which was likened to *Septencoracias* by Mayr and Smith (2019). Therefore, we assign *Microena goodwini* to the Coracii and consider it possible that the roller from the Isle of Sheppey (Mayr and Walsh 2018) belongs to the taxon *Microena*.

Stem group representatives of the Coracii have so far only been reported from the Early Cenozoic of the Northern Hemisphere. As detailed by Mayr (2022b), *Ueenkekcoracias tambussiae* from the early Eocene of Argentina (Degrange et al. 2021) was erroneously assigned to the Coracii and is more likely to be related to the taxon *Palaeopsittacus*, which is a representative of the Strisores (nightjars, swifts, and allies). Another putative South American roller, *Chehuenia facongrandei* from the early-middle Miocene of Argentina (Agnolín 2022), likewise cannot be assigned to the Coracii, because the tarsometatarsus – the only bone known from the species – lacks a plantarly open canalis interosseus distalis; the trochlea metatarsi IV of this species forms a wing-like plantar flange, which also conflicts with its assignment to the Coracii. Stem group Coracii disappeared from North America towards the early Eocene, which was attributed by Mayr (2009: 208) to the disappearance of paratropical rainforests after an onset of climatic cooling in the early Cenozoic. The lack of larger-sized *Eocoracias*- or *Paracoracias*-like stem group Coracii in Walton-on-the-Naze is notable and may either be due to different palaeoecological conditions or indicate that these more crown group-like taxa, which are known from slightly younger fossil sites, were genuinely absent in Europe by the time the London Clay of Walton-on-the-Naze was deposited.

Pristineanis ("*Neanis*") *kistneri* from the North American Green River Formation was assigned to the Piciformes by previous authors (Feduccia 1973; Houde and Olson 1989; Weidig 2010). In this species (GM, pers. obs.) and in the new *Pristineanis* fossils from Walton-on-the-Naze the trochlea metatarsi IV of the tarsometatarsus forms a marked, plantarly directing flange, which indicates at least semizygodactyl feet. A weak sulcus on the distal surface of this trochlea may be homologous to the more pronounced furrow of crown group Piciformes, which separates the trochlea accessoria from the trochlea metatarsi IV and is a distinctive apomorphy of piciform birds. The tarsometatarsus of

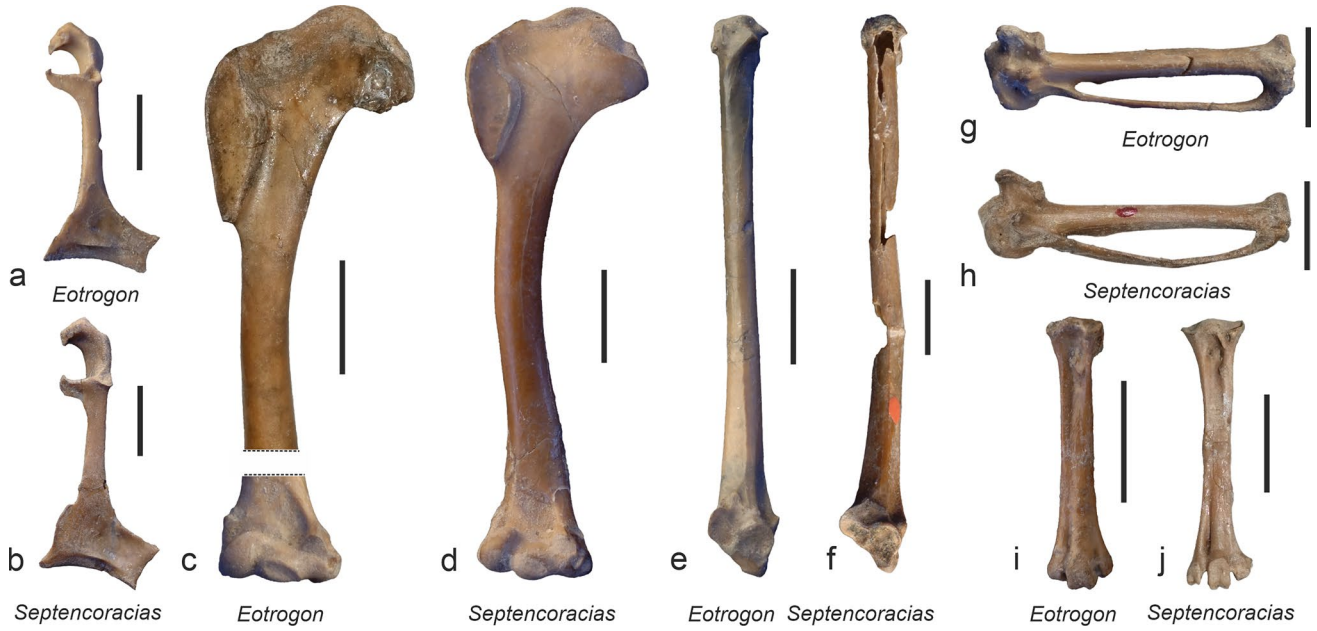

Fig. 9 Comparison of major limb bones of early Eocene stem group Coracii (*Septencoracias*) and stem group Trogoniformes (*Eotrogon*) from Walton-on-the-Naze to illustrate similar sizes, proportions, and morphologies. **a**, **b** right coracoid (dorsal view) of **a** *Eotrogon stenorhynchus* (NMS.Z.2021.40.83) and **b** *Septencoracias morsensis* (NMS.Z.2021.40.144). **c**, **d** right humerus (cranial view) of **c** *E. stenorhynchus* (NMS.Z.2021.40.83; the bone is reconstructed by digitally combining the proximal portion with the mirrored distal end of the left humerus) and **d** *S. simillimus*, sp. nov. (holotype, NMS.Z.2021.40.146). **e**, **f** left ulna (cranial view) of **e** *E. stenorhynchus* (NMS.Z.2021.40.83) and **f** *S. morsensis* (NMS.Z.2021.40.143). **g**, **h** left carpometacarpus of **g** *E. stenorhynchus* (NMS.Z.2021.40.83) and **h** *S. simillimus*, sp. nov. (holotype, NMS.Z.2021.40.146). **i**, **j** right tarsometatarsus of **i** *E. stenorhynchus* (NMS.Z.2021.40.85) and **j** Coracii, gen. et sp. indet. (NMS.Z.2021.40.150). The scale bars equal 5 mm

Pristineanis agrees with that of the Picocoraciades in that it exhibits a crista medianoplantaris, and as in rollers the canalis interosseus distalis is plantarly open. These latter features distinguish it from the superficially similar tarsometatarsus of zygodactyl stem group Passeriformes (Mayr and Kitchener 2023d). A plantarly open canalis interosseus distalis is a characteristic feature of the Coracii, but since the canal is entirely reduced in other representatives of the Picocoraciades, it being plantarly open may be plesiomorphic for the clade. Because the Piciformes are the only zygodactyl representatives of the Picocoraciades and because of previous hypotheses on the affinities of *P. kistneri* (Feduccia 1973; Weidig 2010), we tentatively assign the taxon *Pristineanis* to the Piciformes. However, we note that the morphology of the hypotarsus distinguishes *Pristineanis* from crown group Coraciiformes and Piciformes, in which there is no closed canal for the tendon of musculus flexor hallucis longus, and the hypotarsus morphology of the new taxon corresponds with the Bucerotes, which are the only extant taxon of the Picocoraciades, in which the hypotarsus exhibits two closed canals (Mayr 2016). This hypotarsus morphology may also be plesiomorphic for the Picocoraciades.

The representatives of the Bucerotes and Coracii already showed quite disparate morphologies by the early Eocene, 55 Ma, so that the major groups of the Picocoraciades probably diverged well before that date. In many aspects of their postcranial osteology, the stem group Coracii from Walton-on-the-Naze resemble the coeval *Eotrogon stenorhynchus* from this fossil site, which is the earliest well-represented trogoniform bird (Fig. 9; Mayr et al. 2023). As noted above, the coracoid of *Pristineanis* likewise closely corresponds to that of *E. stenorhynchus*. The Trogoniformes are the extant sister taxon of the Picocoraciades (e.g., Prum et al. 2015; Kuhl et al. 2021), and the shared similarities of *Eotrogon* and the Coracii from the London Clay are therefore likely to be plesiomorphic for the Picocoraciades and shed light on the ancestral morphology of Eucavitaves, the clade including the Picocoraciades and the Trogoniformes (Sangster et al. 2022). Because many taxa of the Eucavitaves nest in self-excavated burrows or tree cavities, functional correlations may exist between their breeding biology and skeletal morphology.

All early Cenozoic representatives of the Upupiformes and most stem group Coracii were much smaller than their extant relatives. It was first proposed Mayr (2017: 92f., 204f.) that the radiation of arboreal neornithine birds took place after global deforestation at the K/Pg boundary, which led to the extinction of the Mesozoic Enantiornithes (this hypothesis was subsequently captured by Field et al. 2018 without reference to the former study). The fossil birds from

the London Clay of Walton-on-the-Naze are only 10 million years younger than the K/Pg boundary, so that a small size is likely to be plesiomorphic for the Picocoraciades. In this case, the members of the clade would be an avian example of Cope's Rule, which postulates a tendency for size increase in evolutionary lineages over time (e.g., Brown and Maurer 1986; Hone and Benton 2005), and competition for nesting cavities and other ecological resources may have played a role in the multiple parallel size increases within the major lineages of the Picocoraciades.

Acknowledgements We thank Sven Tränkner for taking some of the photographs (additional images are by GM). Comments from two reviewers improved the manuscript. This publication is registered under Zoobank LSID urn:lsid:zoobank.org:pub:30AC939A-780E-4484-9281-A2BA7606AC1A.

Funding Open Access funding enabled and organized by Projekt DEAL.

Data availability All data are included in the paper.

Declarations

Conflict of interest The authors declare no conflict of interest.

References

Agnolín, F.L. 2022. New fossil birds from the Miocene of Patagonia, Argentina. *Poeyana* 513: 1–43.

Aldiss, D.T. 2012. The stratigraphical framework for the Palaeogene successions of the London Basin, UK. *British Geological Survey Open Report* OR/12/004, 1–87.

Bourdon, E., A.V. Kristoffersen, and N. Bonde. 2016. A roller-like bird (Coracii) from the Early Eocene of Denmark. *Scientific Reports* 6: 34050.

Brodkorb, P. 1965. New taxa of fossil birds. *Quarterly Journal of the Florida Academy of Sciences* 28: 197–198.

Brodkorb, P. 1970. An Eocene puffbird from Wyoming. *Contributions to Geology* 9: 13–15.

Brown, J.H., and B.A. Maurer. 1986. Body size, ecological dominance and Cope's rule. *Nature* 324: 248–250.

Chandler, R.M. 1999. Fossil birds of Florissant, Colorado: with a description of a new genus and species of cuckoo. *Geologic Resources Division Technical Report* NPS/NRGRD/GRDTR-99, 49–53.

Clarke, J.A., D.T. Ksepka, N.A. Smith, and M.A. Norell. 2009. Combined phylogenetic analysis of a new North American fossil species confirms widespread Eocene distribution for stem rollers (Aves, Coracii). *Zoological Journal of the Linnean Society* 157: 586–611.

Collinson, M.E., N.F. Adams, S.R. Manchester, G.W. Stull, F. Herrera, S.Y. Smith, M.J. Andrew, P. Kenrick, and D. Sykes. 2016. X-ray micro-computed tomography (micro-CT) of pyrite-permineralized fruits and seeds from the London Clay Formation (Ypresian) conserved in silicone oil: A critical evaluation. *Botany* 94: 697–711.

Degrange, F.J., D. Pol, P. Puerta, and P. Wilf. 2021. Unexpected larger distribution of Paleogene stem-rollers (Aves, Coracii): New evidence from the Eocene of Patagonia, Argentina. *Scientific Reports* 11: 1363.

Dyke, G.J. 2001a. A primitive swift from the London Clay and the relationships of fossil apodiform birds. *Journal of Vertebrate Paleontology* 21: 195–200.

Dyke, G.J. 2001b. *Laputavis*, a replacement name for *Laputa* Dyke 2001 (preoccupied name). *Journal of Vertebrate Paleontology* 21: 401–401.

Feduccia, A. 1973. A new Eocene zygodactyl bird. *Journal of Paleontology* 47: 501–503.

Feduccia, A. 1976. *Neanis schucherti* restudied: Another Eocene piciform bird. *Smithsonian Contributions to Paleobiology* 27: 95–99.

Feduccia, A., and L.D. Martin. 1976. The Eocene zygodactyl birds of North America (Aves: Piciformes). *Smithsonian Contributions to Paleobiology* 27: 101–110.

Field, D.J., A. Bercovici, J.S. Berv, R. Dunn, D.E. Fastovsky, T.R. Lyson, V. Vajda, and J. Gauthier. 2018. Early evolution of modern birds structured by global forest collapse at the end-Cretaceous mass extinction. *Current Biology* 28: 1825–1831.

Forbes, H.O. 1884. Forbes's final idea as to the classification of birds. *Ibis Fifth Series* 2: 119–120.

Fürbringer, M. 1888. *Untersuchungen zur Morphologie und Systematik der Vögel, zugleich ein Beitrag zur Anatomie der Stütz- und Bewegungsorgane*. Amsterdam: Van Holkema.

George, J.C., and A.J. Berger. 1966. *Avian myology*. New York: Academic Press.

Grande, L. 2013. *The Lost World of Fossil Lake. Snapshots from Deep Time*. Chicago: University of Chicago Press.

Harrison, C.J.O., and C.A. Walker. 1977. Birds of the British Lower Eocene. *Tertiary Research Special Papers* 3: 1–52.

Höfling, E., and H.M.F. Alvarenga. 2001. Osteology of the shoulder girdle in the Piciformes, Passeriformes and related groups of birds. *Zoologischer Anzeiger A* 240: 196–208.

Hone, D.W., and M.J. Benton. 2005. The evolution of large size: How does Cope's Rule work? *Trends in Ecology and Evolution* 20: 4–6.

Houde, P., and S.L. Olson. 1989. Small aboreal nonpasserine birds from the Early Tertiary of Western North America. In *Acta congressus internationalis Ornithologici*, ed. H. Ouellet, 2030–2036. Ottawa: University of Ottawa Press.

Jolley, D.W. 1996. The earliest Eocene sediments of eastern England: An ultra-high resolution palynological correlation. *Geological Society London Special Publications* 101: 219–254.

Ksepka, D.T., and J.A. Clarke. 2010. *Primobucco mcgrewi* (Aves: Coracii) from the Eocene Green River Formation: New anatomical data from the earliest constrained record of stem rollers. *Journal of Vertebrate Paleontology* 30: 215–225.

Kuhl, H., C. Frankl-Vilches, A. Bakker, G. Mayr, G. Nikolaus, S.T. Boerno, S. Klages, B. Timmermann, and M. Gahr. 2021. An unbiased molecular approach using 3'UTRs resolves the avian family-level tree of life. *Molecular Biology and Evolution* 38: 108–127.

Linnaeus, C. 1758. *Systema naturae per regna tria naturae*, 10th edition, 2 vols. Holmiae: L. Salmii.

Mayr, G. 1998. "Coraciiforme" und "piciforme" Kleinvögel aus dem Mittel-Eozän der Grube Messel (Hessen, Deutschland). *Courier Forschungsinstitut Senckenberg* 205: 1–101.

Mayr, G. 2000. Tiny hoopoe-like birds from the Middle Eocene of Messel (Germany). *The Auk* 117: 964–970.

Mayr, G. 2001. The relationships of fossil apodiform birds - a comment on Dyke (2001). *Senckenbergiana Lethaea* 81: 1–2.

Mayr, G. 2002. Avian remains from the Middle Eocene of the Geiseltal (Sachsen-Anhalt, Germany). In *Proceedings of the 5th Symposium of the Society of Avian Paleontology and Evolution*, ed. Z. Zhou and F. Zhang, 77–96. Beijing: Science Press.

Mayr, G. 2006. New specimens of the Eocene Messelirrisoridae (Aves: Bucerotes), with comments on the preservation of uropygial gland waxes in fossil birds from Messel and the phylogenetic affinities of Bucerotes. *Paläontologische Zeitschrift* 80: 390–405.

Mayr, G. 2009. *Paleogene fossil birds*. Heidelberg: Springer.

Mayr, G. 2011. Metaves, Mirandornithes, Strisores, and other novelties—a critical review of the higher-level phylogeny of neornithine birds. *Journal of Zoological Systematics and Evolutionary Research* 49: 58–76.

Mayr, G. 2014. Comparative morphology of the radial carpal bone of birds and the phylogenetic significance of character variation. *Zoomorphology* 133: 425–434.

Mayr, G. 2016. Variations in the hypotarsus morphology of birds and their evolutionary significance. *Acta Zoologica* 97: 196–210.

Mayr, G. 2017. *Avian evolution: The fossil record of birds and its paleobiological significance*. Chichester: Wiley-Blackwell.

Mayr, G. 2018. Birds - the most species-rich vertebrate group in Messel. In *Messel—an ancient greenhouse ecosystem*, ed. S.K.F. Schaal, K. Smith, and J. Habersetzer, 169–214. Stuttgart: Schweitzerbart.

Mayr, G. 2020. An updated review of the middle Eocene avifauna from the Geiseltal (Germany), with comments on the unusual taphonomy of some bird remains. *Geobios* 62: 45–59.

Mayr, G. 2022a. *Paleogene fossil birds*, 2nd ed. Cham: Springer.

Mayr, G. 2022b. A partial skeleton of *Septencoracias* from the early Eocene London Clay reveals derived features of bee-eaters (Meropidae) in a putative stem group roller (Aves, Coracii). *Palaeobiodiversity and Palaeoenvironments* 102: 449–463.

Mayr, G., and R. Gregorová. 2012. A tiny stem group representative of Pici (Aves, Piciformes) from the early Oligocene of the Czech Republic. *Paläontologische Zeitschrift* 86: 333–343.

Mayr, G., and A.C. Kitchener. 2023a. New species from the early Eocene London Clay suggest an undetected early Eocene diversity of the Leptosomiformes, an avian clade that includes a living fossil from Madagascar. *Palaeobiodiversity and Palaeoenvironments* 103: 585–608.

Mayr, G., and A.C. Kitchener. 2023b. Early Eocene fossil illuminates the ancestral (diurnal) ecomorphology of owls and documents a mosaic evolution in the strigiform stem lineage. *Ibis* 165: 231–247.

Mayr, G., and A.C. Kitchener. 2023c. The Halcyornithidae from the early Eocene London Clay of Walton-on-the-Naze (Essex, UK): a species complex of Paleogene arboreal birds. *Geobios*. https://doi.org/10.1016/j.geobios.2023.06.003.

Mayr, G., and A.C. Kitchener. 2023d. Psittacopedids and zygodactylids: The diverse and species-rich psittacopasserine birds from the early Eocene London Clay of Walton-on-the-Naze (Essex, UK). *Historical Biology* 35: 2372–2395.

Mayr, G., and C. Mourer-Chauviré. 2000. Rollers (Aves: Coraciiformes s.s.) from the Middle Eocene of Messel (Germany) and the Upper Eocene of the Quercy (France). *Journal of Vertebrate Paleontology* 20: 533–546.

Mayr, G., and T. Smith. 2013. Galliformes, Upupiformes, Trogoniformes, and other avian remains (?Phaethontiformes and ?Threskiornithidae) from the Rupelian stratotype in Belgium with comments on the identity of "*Anas*" *benedeni* Sharpe. In *Paleornithological Research 2013—Proceedings of the 8th International Meeting of the Society of Avian Paleontology and Evolution*, ed. U.B. Göhlich and A. Kroh, 23–35. Vienna: Natural History Museum.

Mayr, G., and T. Smith. 2019. A diverse bird assemblage from the Ypresian of Belgium furthers knowledge of early Eocene avifaunas of the North Sea Basin. *Neues Jahrbuch für Geologie und Paläontologie, Abhandlungen* 291: 253–281.

Mayr, G., and S. Walsh. 2018. Exceptionally well-preserved early Eocene fossil reveals cranial and vertebral features of a stem group roller (Aves, Coraciiformes). *Paläontologische Zeitschrift* 92: 715–726.

Mayr, G., C. Mourer-Chauviré, and I. Weidig. 2004. Osteology and systematic position of the Eocene Primobucconidae (Aves, Coraciiformes sensu stricto), with first records from Europe. *Journal of Systematic Palaeontology* 2: 1–12.

Mayr, G., Z.M. Bochenski, T. Tomek, K. Wertz, M. Bienkowska-Wasiluk, and A. Manegold. 2020. Skeletons from the early Oligocene of Poland fill a significant temporal gap in the fossil record of upupiform birds (hoopoes and allies). *Historical Biology* 32: 1163–1175.

Mayr, G., V.L. De Pietri, and A.C. Kitchener. 2023. Narrow-beaked trogons from the early Eocene London Clay of Walton-on-the-Naze (Essex, UK). *Journal of Ornithology* 164: 749–764.

Meyer, B., and J. Wolf. 1810. *Taschenbuch der deutschen Vögelkunde oder kurze Beschreibung aller Vögel Deutschlands*. Frankfurt am Main: F. Wilmans.

Prum, R.O., J.S. Berv, A. Dornburg, D.J. Field, J.P. Townsend, E.M. Lemmon, and A.R. Lemmon. 2015. A comprehensive phylogeny of birds (Aves) using targeted next-generation DNA sequencing. *Nature* 526: 569–573.

Rayner, D., T. Mitchell, M. Rayner, and F. Clouter. 2009. *London Clay fossils of Kent and Essex*. Rochester, Kent: Medway Fossil and Mineral Society.

Sangster, G., E.L. Braun, U.S. Johansson, R.T. Kimball, G. Mayr, and A. Suh. 2022. Phylogenetic definitions for 25 higher-level clade names of birds. *Avian Research* 13: 100027.

Seebohm, H. 1890. *The birds of the Japanese Empire*. London: R.H. Porter.

Shufeldt, R.W. 1913. Fossil feathers and some heretofore undescribed fossil birds. *Journal of Geology* 21: 628–652.

Stegmann, B. 1965. Funktionell bedingte Eigenheiten am Metacarpus des Vogelflügels. *Journal für Ornithologie* 106: 179–189.

Watanabe, J., D.J. Field, and H. Matsuoka. 2021. Wing musculature reconstruction in extinct flightless auks (*Pinguinus* and *Mancalla*) reveals incomplete convergence with penguins (Spheniscidae) due to differing ancestral states. *Integrative Organismal Biology* 3: 040.

Weidig, I. 2010. New birds from the lower Eocene Green River Formation, North America. *Records of the Australian Museum* 62: 29–44.

Wetmore A, Miller WW. 1926. The revised classification for the fourth edition of the AOU Check-list. *The Auk* 43: 337–346.